Perturbative and Geometric Analysis of the Quartic Kontsevich Model

Johannes BRANAHL [a], Alexander HOCK [b] and Raimar WULKENHAAR [a]

a) *Mathematisches Institut, Westfälische Wilhelms-Universität Münster,*
   Einsteinstr. 62, 48149 Münster, Germany
   E-mail: *j_bran33@uni-muenster.de, raimar@math.uni-muenster.de*
   URL: https://www.uni-muenster.de/MathPhys/

b) *Mathematical Institute, University of Oxford,*
   Andrew Wiles Building, Woodstock Road, OX2 6GG, Oxford, UK
   E-mail: *alexander.hock@maths.ox.ac.uk*

Abstract. The analogue of Kontsevich's matrix Airy function, with the cubic potential $\mathrm{Tr}\left(\Phi^3\right)$ replaced by a quartic term $\mathrm{Tr}\left(\Phi^4\right)$ with the same covariance, provides a toy model for quantum field theory in which all correlation functions can be computed exactly and explicitly. In this paper we show that distinguished polynomials of correlation functions, themselves given by quickly growing series of Feynman ribbon graphs, sum up to much simpler and highly structured expressions. These expressions are deeply connected with meromorphic forms conjectured to obey blobbed topological recursion. Moreover, we show how the exact solutions permit to explore critical phenomena in the quartic Kontsevich model.

Key words: Dyson–Schwinger equations; perturbation theory; exact solutions; topological recursion

2020 Mathematics Subject Classification: 81T18; 81T16; 14H81; 32A20

Dedicated to Dirk Kreimer
on the occasion of his 60th birthday

1 Introduction

Quantum field theory has often been a source of inspiration for mathematics. In the previous 25 years, many of these inspirations came from Dirk Kreimer. We mention the vision [28] of a deep relation between Feynman graphs and knots which led to impressive progress on multiple zeta values [12]. The discovery that renormalisation in quantum field theory is encoded in a Hopf algebra [29] led to the insight that renormalisation is another example for the Birkhoff decomposition to solve a Riemann–Hilbert problem [15]. There is much more to say, but we confine ourselves to highlighting just one point: Although the Hopf algebra was originally defined with Feynman graphs, it was emphasised very soon [13] that Dyson–Schwinger equations will eventually provide a non-perturbative formulation.

One may ask whether multiple zeta values and other connections between quantum field theory and number theory also find a non-perturbative explanation. We are working on a programme which achieves and investigates the exact solution of a quantum field theory toy model, namely of a matrix model with quartic interaction and non-trivial covariance [24]. It is already

known that for particular choices of parameters the exact solution of the planar sector expands into number-theoretic objects such as Nielsen polylogarithms [31] and hyperlogarithms [22], respectively.

It is highly desirable to extend this construction to richer topological sectors, which can be seen as analogy to knots. This contribution provides the first steps in this direction. We give a low-order perturbative expansion of exact correlation functions, derived in [10], and compare the result with a Feynman graph evaluation. We perform this investigation in a finite-dimensional case where no renormalisation is needed. We show that even this simple case has rich features, for instance an enormous simplification in particular polynomials of correlation functions (or Feynman graphs) compared with individual functions or graphs. We expect that these simplifications will extend to an infinite-dimensional limit where renormalisation is necessary, although considerable work is still ahead.

2   The model

We sketch the main ideas about the model under consideration and refer to [10, 32] for more details. We follow the paragon of the $\lambda\phi^4$ model, but defined on a noncommutative space instead of on a Riemannian or Lorentzian manifold. Apart from physical reasons, choosing a noncommutative geometry has the advantage of a simple finite-dimensional approximation. Let H_N be the real vector space of self-adjoint $(N \times N)$-matrices, H'_N be its dual and (e_{kl}) be the standard matrix basis in the complexification of H_N. Our quantum scalar fields are noncommutative random variables Φ on H'_N distributed according to a measure

$$
\mathrm{d}\mu_{E,\lambda}(\Phi) = \frac{1}{\mathcal{Z}} \exp\left(-\frac{\lambda N}{4} \operatorname{Tr}\left(\Phi^4\right)\right) \mathrm{d}\mu_{E,0}(\Phi),
$$
$$
\mathcal{Z} := \int_{H'_N} \exp\left(-\frac{\lambda N}{4} \operatorname{Tr}\left(\Phi^4\right)\right) \mathrm{d}\mu_{E,0}(\Phi),
\tag{2.1}
$$

where $\mathrm{d}\mu_{E,0}(\Phi)$ is a Gaußian measure with covariance $\left[\int_{H'_N} \mathrm{d}\mu_{E,0}(\Phi)\, \Phi(e_{jk})\Phi(e_{lm})\right]_c = \frac{\delta_{jm}\delta_{kl}}{N(E_j+E_l)}$ for some $0 < E_1 < \cdots < E_N$. We call the Euclidean quantum field theory defined via (2.1) the *quartic Kontsevich model* because of its formal analogy with the Kontsevich model [27] in which $\frac{\lambda}{4} \operatorname{Tr}\left(\Phi^4\right)$ in (2.1) is replaced by[1] $\frac{\mathrm{i}}{6} \operatorname{Tr}\left(\Phi^3\right)$. The Gaußian measure $\mathrm{d}\mu_{E,0}(\Phi)$ is the same. Kontsevich proved in [27] that (2.1) with $\operatorname{Tr}\left(\Phi^3\right)$-term, viewed as function of the E_k, is the generating function for intersection numbers of tautological characteristic classes on the moduli space $\overline{\mathcal{M}}_{g,n}$ of stable complex curves.

Derivatives of the Fourier transform $\mathcal{Z}(M) := \int_{H'_N} \mathrm{d}\mu_{E,\lambda}(\Phi) \mathrm{e}^{\mathrm{i}\Phi(M)}$ with respect to matrix entries M_{kl} and parameters E_k of the free theory give rise to *Dyson–Schwinger equations* between the cumulants

$$
\langle e_{k_1 l_1} \cdots e_{k_n l_n} \rangle_c = \frac{1}{\mathrm{i}^n} \frac{\partial^n \log \mathcal{Z}(M)}{\partial M_{k_1 l_1} \cdots \partial M_{k_n l_n}}\bigg|_{M=0}.
\tag{2.2}
$$

Of particular interest are cumulants of the form

$$
N^{n_1+\cdots+n_b} \big\langle (e_{k_1^1 k_2^1} e_{k_2^1 k_3^1} \cdots e_{k_{n_1}^1 k_1^1}) \cdots (e_{k_1^b k_2^b} e_{k_2^b k_3^b} \cdots e_{k_{n_b}^b k_1^b}) \big\rangle_c
$$
$$
=: N^{2-b} \, G_{|k_1^1 \cdots k_{n_1}^1| \cdots |k_1^b \cdots k_{n_b}^b|},
\tag{2.3}
$$

---

[1] In the Kontsevich model with potential $\operatorname{Tr}\left(\Phi^3\right)$, a purely imaginary coupling constant is necessary for convergence of $\mathcal{Z}$. Of course, $\mathrm{d}\mu_{E,\lambda}$ is then only a signed measure. Choosing $\lambda > 0$ in the quartic model with potential $\operatorname{Tr}\left(\Phi^4\right)$ gives both a convergent partition function $\mathcal{Z}$ and a true measure $\mathrm{d}\mu_{E,\lambda}$.

called $(n_1 + \cdots + n_b)$-point functions. To define these functions properly it is necessary that the k_i^j are pairwise different. After their identification a natural extension to any diagonal is possible. The corresponding derivatives in (2.2) then decompose into linear combinations of such functions. One has, for example, $-N^2 \frac{\partial^2 \log \mathcal{Z}(M)}{\partial M_{kk} \partial M_{kk}} = N G_{|kk|} + G_{|k|k|}$.

After $1/N$-expansion $G_{|k_1^1 \cdots k_{n_1}^1| \cdots |k_1^b \cdots k_{n_b}^b|} =: \sum_{g=0}^{\infty} N^{-2g} G_{|k_1^1 \cdots k_{n_1}^1| \cdots |k_1^b \cdots k_{n_b}^b|}^{(g)}$ of the correlation functions (2.3) one obtains a non-linear equation for the planar 2-point function $G_{|kl|}^{(0)}$ alone [23] and a hierarchy of affine equations for all other functions. The arduous solution process for $G_{|kl|}^{(0)}$ was recently completed in [21, 31].

Then things accelerated: During the attempt of finding an elegant algorithm to cover any correlation function, we recognised that we were somehow looking for the wrong quantities: A non-trivial rearrangement [10] of those gives birth to meromorphic differential forms $\omega_{g,n}$ labelled by genus g and number n of marked points of a Riemann surface. The solution of the complicated Dyson–Schwinger equations for $\omega_{g,n}$ at small $2g + n - 2$ in [10] provided strong evidence[2] for a remarkable algebraic structure behind the model under consideration: (*blobbed*) [5] *topological recursion* [18]. As a consequence, the $\omega_{g,n}$ with $2g + n - 2 < 0$ are recursively built from $\omega_{0,1}$ and $\omega_{0,2}$ by a relatively simple evaluation of residues, much faster than solving the Dyson–Schwinger equations. Topological recursion has been identified in numerous areas of mathematics and physics including one- and two-matrix models [14], Hurwitz theory [9] and Gromov–Witten theory [8]. Topological recursion also governs the combinatorics of the Kontsevich model [27] (see, e.g., [17, Chapter 6] for details) and organises the Weil–Petersson volumes of moduli spaces of hyperbolic Riemann surfaces [30].

We discuss in Section 3 the perturbative expansion of correlation functions (2.3) into weighted labelled ribbon graphs. Section 4 shows that two families of auxiliary functions $T^{(g)}$ and $\Omega^{(g)}$ introduced in [10] are representable as polynomials in correlation functions. Section 5 compares the Taylor series of exact results for $\Omega^{(g)}$ with the ribbon graph expansion of the correlation functions. It is impressive to see how contributions of a huge number of ribbon graphs almost cancel up to a tiny and structured remnant which is conjectured to obey blobbed topological recursion. In Section 6 we start a (partly numerical) investigation of critical phenomena in the quartic Kontsevich model. The number of branch cuts and the order of ramification points changes at critical values of the coupling constant. Interestingly, the correlation functions cross analytically into the other phases. We conclude in Section 7 with possible lessons for more realistic quantum field theories.

2.1 Differences between the quartic Kontsevich model and the generalised Kontsevich model

The notation of the generalised Kontsevich model (GKM) is well-defined in the literature. The original motivation came from Witten [33] in terms of the r-spin classes on the moduli space of complex curves, $r \in \mathbb{N}_{>1}$. Also the corresponding formal matrix model representation is well-known [1]. Its partition function is defined by [2]

$$\mathcal{Z}^{\text{rspin}} := \int_{H_N} \mathrm{d}M \mathrm{e}^{-N\alpha^{r+1}\operatorname{Tr}(V(M)-V(\Lambda)-(M-\Lambda)V'(\Lambda))}, \tag{2.4}$$

where $V(M) = \frac{M^{r+1}}{r+1}$ is the potential, α a formal parameter and Λ the diagonal matrix with positive eigenvalues $\Lambda_1, \ldots, \Lambda_N$.

---

[2] Two of us have proved the algebraic structure of blobbed topological recursion for the genus $g = 0$ case in [26].

In case of $r = 2$, this model becomes exactly the Kontsevich model [27]

$$\mathcal{Z}^{2\text{spin}} = \int_{H_N} \mathrm{d}M \mathrm{e}^{-N\alpha^3 \operatorname{Tr}\left(\frac{M^3}{3} - M\Lambda^2 + \frac{2\Lambda^3}{3}\right)} = \int_{H_N} \mathrm{d}\tilde{M} \mathrm{e}^{-N\alpha^3 \operatorname{Tr}\left(\frac{\tilde{M}^3}{3} + \tilde{M}^2\Lambda\right)}$$

with the transformation $M = \tilde{M} + \Lambda$ in the last equality. The last representation in terms of $\tilde{M}$ leads to the combinatorics of weighted ribbon graphs with 3-valent vertices (see Section 3).

However, avoiding for $r > 2$ the linear term in M in the exponential in (2.4) by a transformation $M = \tilde{M} + \Lambda$ one gets a very restricted matrix model. For instance, the $r = 3$ case is

$$\mathcal{Z}^{3\text{spin}} = \int_{H_N} \mathrm{d}M \mathrm{e}^{-N\alpha^4 \operatorname{Tr}\left(\frac{M^4}{4} - M\Lambda^3 + \frac{3\Lambda^4}{4}\right)} = \int_{H_N} \mathrm{d}\tilde{M} \mathrm{e}^{-N\alpha^4 \operatorname{Tr}\left(\frac{\tilde{M}^4}{4} + \tilde{M}^3\Lambda + \frac{3}{2}\tilde{M}^2\Lambda^2\right)}. \tag{2.5}$$

We emphasise that the r-spin matrix model is proved to satisfy topological recursion for the combinatorics of the resolvents [19]. Also for the expectation values of disjoint cycles it is proved in [2] that it is governed by higher topological recursion of Bouchard and Eynard [6]. These two results are connected by exchanging the rôle of x and y in topological recursion.

Now, the model considered in this paper, defined via (2.1) and the same covariance as the Kontsevich model, has the following matrix model representation, achieved by the canonical duality between the vector space H_N and its dual H_N':

$$\mathcal{Z} = \int_{H_N} \mathrm{d}\tilde{M} \, \mathrm{e}^{-N \operatorname{Tr}\left(\frac{\lambda \tilde{M}^4}{4} + \frac{1}{2}\tilde{M}^2 E\right)},$$

where the diagonal matrix E has the entries $0 < E_1 < \cdots < E_N$.

We see that the quartic Kontsevich model does not fit into the class of r-spin models, even for arbitrary polynomial potentials in (2.4). For instance, the cubic term of $\tilde{M}$ in (2.5) is also weighted by the external matrix Λ and its appearance is indispensable. It turns out that the more complicated enumerative structure of r-spin models has the easier algebraic structure in terms of (higher-order) topological recursion, whereas the easier enumerative structure of the quartic Kontsevich model is governed by the enriched structure of blobbed topological recursion.

In the subsequent section, the combinatorics of the quartic Kontsevich model is discussed. For the combinatorics of the r-spin model we refer to the recent work [2].

3 Perturbation theory

3.1 Weighted labelled ribbon graphs

The expansion of $\exp\left(-\frac{\lambda N}{4} \operatorname{Tr}\left(\Phi^4\right)\right)$ inside the measure $\mathrm{d}\mu_{E,\lambda}(\Phi)$ defined in (2.1) represents the cumulants (2.2) as a series

$$\begin{aligned}
&\langle e_{p_1 q_1} \cdots e_{p_n q_n} \rangle_c \\
&= \sum_{v=0}^{\infty} \frac{N^v (-\lambda)^v}{4^v v!} \left[\int_{H_N'} \mathrm{d}\mu_{E,0}(\Phi) \Phi_{p_1 q_1} \cdots \Phi_{p_n q_n} \sum_{j_1,\ldots,m_v=1}^{N} \prod_{i=1}^{v} \left(\Phi_{j_i k_i} \Phi_{k_i l_i} \Phi_{l_i m_i} \Phi_{m_i j_i} \right) \right]_c, \tag{3.1}
\end{aligned}$$

where $\Phi_{kl} := \Phi(e_{kl})$ and $[\ ]_c$ means taking the connected part. We fix the order v and restrict our attention to the case that $p_1,\ldots,p_n$ are pairwise different. By the definition of the Gaußian measure $\mathrm{d}\mu_{E,0}(\Phi)$, this integral is zero for n odd, whereas for n even it evaluates into a sum over all partitions of $\Phi_{p_1 q_1} \cdots \Phi_{p_n q_n} \sum_{j_1,\ldots,m_v=1}^{N} \prod_{i=1}^{v} \left(\Phi_{j_i k_i} \Phi_{k_i l_i} \Phi_{l_i m_i} \Phi_{m_i j_i} \right)$ into products of pairs with a pair $(\Phi_{jk} \Phi_{lm})$ replaced by $\frac{\delta_{jm} \delta_{kl}}{N(E_j + E_l)}$.

Every pairing contributing to (3.1) has a convenient visualisation as a ribbon graph. Its building blocks are n one-valent vertices representing $\Phi_{p_1 q_1}, \ldots, \Phi_{p_n q_n}$ and v four-valent vertices representing $\Phi_{j_i k_i} \Phi_{k_i l_i} \Phi_{l_i m_i} \Phi_{m_i j_i}$ for $i = 1, \ldots, v$ as well as r ribbons which connect the vertices. A ribbon represents a pair $(\Phi_{jk} \Phi_{lm})$; it is drawn as a double line $\frac{\quad l \quad}{\quad j \quad}$ between the vertices (can be the same) at which Φ_{jk} and Φ_{lm} are located. The two strands of this double line are labelled j and l, respectively. A strand is left open at a one-valent vertex, whereas at a four-valent vertex we connect it with the strand of the neighboured ribbon. A four-valent vertex with its attached ribbons thus looks as $\frac{m|\,|l}{j|\,|k}$. A ribbon graph is connected when any two vertices (one- or four-valent) are connected by a chain of ribbons. We only retain the connected ribbon graphs in (3.1).
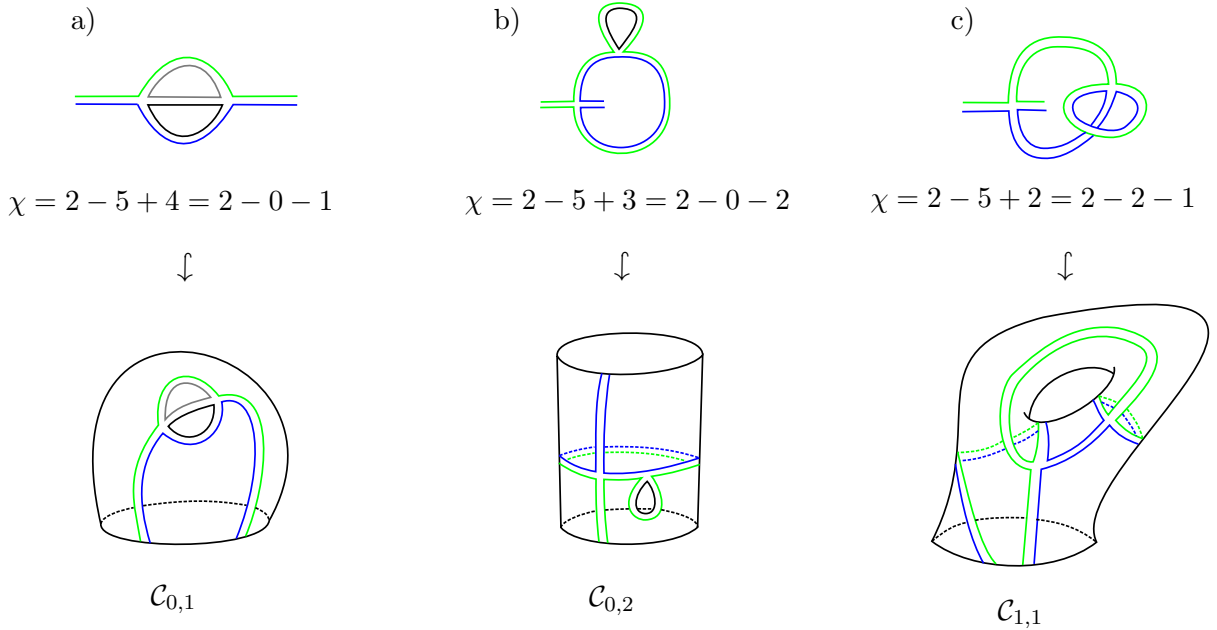

a) $\chi = 2 - 5 + 4 = 2 - 0 - 1$

b) $\chi = 2 - 5 + 3 = 2 - 0 - 2$

c) $\chi = 2 - 5 + 2 = 2 - 2 - 1$

$\mathcal{C}_{0,1}$ $\qquad$ $\mathcal{C}_{0,2}$ $\qquad$ $\mathcal{C}_{1,1}$

Figure 1. Three different ribbon graphs together with the associated Riemann surfaces $\mathcal{C}_{g,b}$. The external strands are coloured in green and blue. The topology of $\mathcal{C}_{g,b}$ is computed by $\chi = v - r + (n+s) = 2 - 2g - b$.

The upper row of Figure 1 shows three examples of ribbon graphs with $n = 2$ one-valent vertices, $v = 2$ four-valent vertices and $r = 5$ ribbons. In general, this construction lets the strands connect to n open lines and a certain number s loops. Due to the Kronecker-δs from pairs and vertices, every one of the $n + s$ lines or loops carries a unique label. Every loop is labelled by a summation index which is the remnant of the summation $\sum_{j_1, \ldots, m_v = 1}^{N}$ in (3.1) after taking all Kronecker-δs into account. The open lines are labelled by the first matrix indices $p_1, \ldots, p_n$ of the product $\Phi_{p_1 q_1} \cdots \Phi_{p_n q_n}$ in (3.1), and the integral (3.1) is zero unless there is a permutation $\pi \in \mathcal{S}_n$ with $q_i = \pi(p_i)$ for all $i = 1, \ldots, n$. This permutation π is uniquely[3] determined by the ribbon graph, simply by looking at the strand labels of the ribbon at every one-valent vertex.

Next, observe that due to the symmetry of the product $\prod_{i=1}^{v} \left(\Phi_{j_i k_i} \Phi_{k_i l_i} \Phi_{l_i m_i} \Phi_{m_i j_i} \right)$ in (3.1) under cyclic permutation $j_i \to k_i \to l_i \to m_i \to j_i$ of order 4 at every vertex and the $v!$ permutations of the vertices there are $4^v v!$ pairings which give the same labelled ribbon graph. We can thus omit the factor $\frac{1}{4^v v!}$ and sum only over the different labelled ribbon graphs. This expresses the integral (3.1) as follows:

---

[3] Uniqueness of π is the reason for choosing $p_1, \ldots, p_n$ pairwise different.

Proposition 3.1. *Let $p_1, \ldots, p_n$ be pairwise different and $\mathfrak{G}^{v,\pi}_{p_1,\ldots,p_n}$ be the set of labelled connected ribbon graphs with v four-valent vertices and n one-valent vertices labelled $(p_1, \pi(p_1)), \ldots, (p_n, \pi(p_n))$. Then for n even the integral* (3.1) *evaluates to*

$$N^n \langle e_{p_1 \pi(p_1)} \cdots e_{p_n \pi(p_n)} \rangle_c = \sum_{v=0}^{\infty} \sum_{\Gamma \in \mathfrak{G}^{v,\pi}_{p_1,\ldots,p_n}} N^{v-r+n+s(\Gamma)} \varpi(\Gamma), \qquad (3.2)$$

where $r = 2v + n/2$ is the number of ribbons, $s(\Gamma)$ the number of loops in Γ and the weight $\varpi(\Gamma)$ is derived from the following Feynman rules:

- *label the $s = s(\Gamma)$ loops by $k_1, \ldots, k_s$;*

- *associate a factor $-\lambda$ to a 4-valent ribbon-vertex;*

- *associate the factor $\frac{1}{E_p + E_q}$ to a ribbon with strands labelled by p, q;*

- *multiply all factors and apply the summation operator $\frac{1}{N^s} \sum_{k_1,\ldots,k_s=1}^{N}$.*

The exponent $\chi := v - r + n + s(\Gamma)$ of N in (3.2) has a topological interpretation. Let b be the number of cycles in π. We take b auxiliary faces, called boundary components, and attach the one-valent vertices in cyclic order and according to the cycle they belong to the circumference of the boundary components. The edge between two neighboured vertices on a boundary component closes an open line of Γ. In total this produces n additional loops. We thus get a simplicial 2-complex of $v + n$ vertices, $r + n$ edges and $b + n + s$ faces, hence of Euler characteristic $2 - 2g = (v + n) - (r + n) + (b + n + s)$. This identifies the exponent $\chi = 2 - 2g - b = v - r + n + s$ of N as the Euler characteristic of a bordered Riemann surface $\mathcal{C}_{g,b}(\Gamma)$. It is, up to homotopy, uniquely defined[4] by the simplicial 2-complex encoded in Γ. The lower row of Figure 1 sketches the bordered Riemann surfaces defined by the corresponding ribbon graphs of the first row.

To compare with the solution via Dyson–Schwinger equations we give an equivalent formulation of (3.2). A ribbon graph $\Gamma \in \mathfrak{G}^{v,\pi}_{p_1,\ldots,p_n}$ contains full information about the cycle type of $\pi \in \mathcal{S}_n$ and about which of the $p_1, \ldots, p_n$ label a chosen cycle of π. We rearrange these labels as follows. Set $p^1_1 := p_1$ and then recursively $p^1_k := \pi^{1-k}(p^1_1)$ for $k = 2, \ldots, n_1$ if $\pi^{-n_1}(p^1_1) = p^1_1$. Next relabel any of the not yet assigned p_k as p^2_1 and continue to set $p^2_k := \pi^{1-k}(p^2_1)$ for $k = 2, \ldots, n_2$ if $\pi^{-n_2}(p^2_1) = p^2_1$. Proceed until the relabelling is complete. We denote by $\mathfrak{G}^{v}_{|p^1_1 \cdots p^1_{n_1}| \cdots |p^b_1 \cdots p^b_{n_b}|}$ the set of relabelled ribbon graphs in $\mathfrak{G}^{v,\pi}_{p_1,\ldots,p_n}$; both sets are in one-to-one correspondence. We further partition this set as $\mathfrak{G}^{v}_{|p^1_1 \cdots p^1_{n_1}| \cdots |p^b_1 \cdots p^b_{n_b}|} = \bigcup_{g=0}^{\infty} \mathfrak{G}^{g,v}_{|p^1_1 \cdots p^1_{n_1}| \cdots |p^b_1 \cdots p^b_{n_b}|}$ into subsets of graphs of the same genus g. For fixed v, this union is actually finite. With these preparations we can represent the series coefficients of the genus expansion

$$G_{|p^1_1 \cdots p^1_{n_1}| \cdots |p^b_1 \cdots p^b_{n_b}|} = \sum_{g=0}^{\infty} N^{-2g} G^{(g)}_{|p^1_1 \cdots p^1_{n_1}| \cdots |p^b_1 \cdots p^b_{n_b}|}$$

of (2.3) for pairwise different $p^j_i \in \{1, \ldots, N\}$ as

$$G^{(g)}_{|p^1_1 \cdots p^1_{n_1}| \cdots |p^b_1 \cdots p^b_{n_b}|} = \sum_{v=0}^{\infty} \sum_{\Gamma \in \mathfrak{G}^{g,v}_{|p^1_1 \cdots p^1_{n_1}| \cdots |p^b_1 \cdots p^b_{n_b}|}} \varpi(\Gamma).$$

---

[4]The dual graph of a connected ribbon graph Γ associated to $\mathcal{C}_{g,b}$ is a quadrangulation (a map) of $\mathcal{C}_{g,b}$. Our definition of the correlation functions by disjoint cycles is equivalent to the definition used in [4] for fully simple maps. Fully simple maps are a subset of ordinary maps which are usually studied in matrix models (see [4] for more details).

Remark 3.2. One can define similar structures for the logarithm of the partition function itself,

$$\log \mathcal{Z} = \log \int_{H'_N} \mathrm{d}\mu_{E,0}(\Phi) \, \mathrm{e}^{-\frac{\lambda N}{4} \operatorname{Tr}(\Phi^4)}.$$

Let $\mathfrak{G}^{g,v}_{\varnothing}$ be the set of connected vacuum ribbon graphs of genus g made of v four-valent vertices and no one-valent vertices. Then the analogue of (3.2) is

$$\log \mathcal{Z} = \sum_{g=0}^{\infty} \sum_{v=0}^{\infty} \sum_{\Gamma_0 \in \mathfrak{G}^{g,v}_{\varnothing}} \frac{N^{2-g} \varpi(\Gamma_0)}{|\mathrm{Aut}(\Gamma_0)|},$$

where $\varpi(\Gamma_0)$ is given by the same Feynman rules as in Proposition 3.1 and $|\mathrm{Aut}(\Gamma_0)|$ is the order of the automorphism group[5] of the vacuum ribbon graph Γ_0.

Later in Definition 4.1 we will introduce the free energy. We can perturbatively establish

$$\mathcal{F}^{(g)} = -\frac{\delta_{g,0}}{2N^2} \sum_{k,l=1}^{N} \log(E_k + E_l) + \sum_{v=1}^{\infty} \sum_{\Gamma_0 \in \mathfrak{G}^{g,v}_{\varnothing}} \frac{\varpi(\Gamma_0)}{|\mathrm{Aut}(\Gamma_0)|}. \tag{3.3}$$

3.2　Examples

Example 3.3. For the ribbon graphs of Figure 1, we label the green open line by p_1 and the blue open line by p_2. Consequently, the graphs become elements of $\mathfrak{G}^{0,2}_{|p_1 p_2|}$, $\mathfrak{G}^{0,2}_{|p_1|p_2|}$, $\mathfrak{G}^{1,2}_{|p_1 p_2|}$ respectively. The weights $\varpi(\Gamma)$ associated to these ribbon graphs are

a)　$\dfrac{(-\lambda)^2}{N^2(E_{p_1} + E_{p_2})^2} \displaystyle\sum_{k_1,k_2=1}^{N} \dfrac{1}{(E_{p_1} + E_{k_1})(E_{p_2} + E_{k_2})(E_{k_1} + E_{k_2})}$,

b)　$\dfrac{(-\lambda)^2}{N(E_{p_1} + E_{p_2})^2(2E_{p_1})(2E_{p_2})} \displaystyle\sum_{k_1=1}^{N} \dfrac{1}{E_{p_1} + E_{k_1}}$,

c)　$\dfrac{(-\lambda)^2}{(E_{p_1} + E_{p_2})^3(2E_{p_1})(2E_{p_2})}$.

Example 3.4. The free energy $\mathcal{F}^{(0)}$ of genus $g = 0$ consists of the empty ribbon graph with weight given by the first term in (3.3) and 4 ribbon graphs up to order λ^2 (see Figure 2). Taking weights and order of the automorphism groups into account, we have perturbatively

$$\mathcal{F}^{(0)} = \frac{-1}{2N^2} \sum_{k,l=1}^{N} \log(E_k + E_l) + \frac{(-\lambda)}{2N^3} \sum_{k,l,m=1}^{N} \frac{1}{(E_k + E_l)(E_k + E_m)}$$

$$+ \frac{(-\lambda)^2}{2N^4} \sum_{j,k,l,m=1}^{N} \frac{1}{(E_j + E_m)(E_j + E_k)^2} \left(\frac{1}{E_j + E_l} + \frac{1}{E_k + E_l} \right)$$

$$+ \frac{(-\lambda)^2}{8N^4} \sum_{j,k,l,m=1}^{N} \frac{1}{(E_j + E_k)(E_k + E_l)(E_l + E_m)(E_m + E_j)} + \mathcal{O}(\lambda^3).$$

---

[5] The automorphism group of any ribbon graph Γ with at least one boundary $b \geq 1$ is trivial, i.e., $|\mathrm{Aut}(\Gamma)| = 1$.
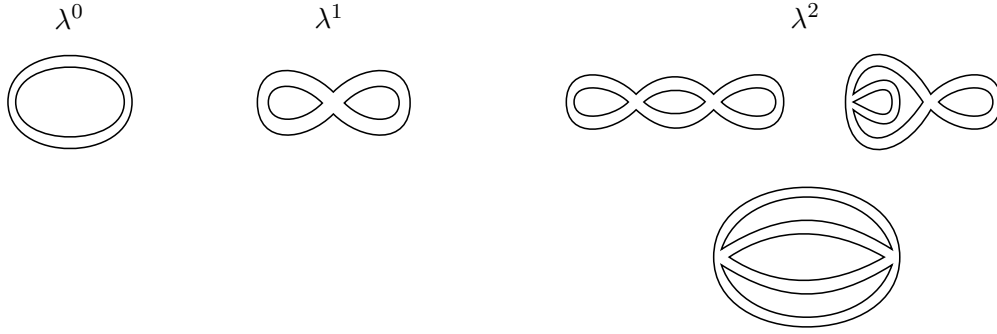
Figure 2. The graph at order λ^0 is added as the empty ribbon graph. All these graphs contribute to the free energy of genus 0 up to order λ^2. These graphs are elements of $\mathfrak{G}_{\varnothing}^{0,v}$. The melon graph Γ_M (in the second row) has $|\text{Aut}(\Gamma_M)| = 8$ and the other four graphs $|\text{Aut}(\Gamma)| = 2$.

Example 3.5. The first example with one boundary component is the 2-point function to which 12 ribbon graphs contribute up to order λ^2 (see Figure 3). Taking the weights into account, we have perturbatively

$$
\begin{aligned}
G_{|ab|}^{(0)} = {} & \frac{1}{E_a + E_b} + \frac{(-\lambda)}{(E_a + E_b)^2} \frac{1}{N} \sum_{k=1}^{N} \left(\frac{1}{E_a + E_k} + \frac{1}{E_b + E_k} \right) \\
& + \frac{(-\lambda)^2}{(E_a + E_b)^2} \frac{1}{N^2} \sum_{k,l=1}^{N} \left(\frac{1}{(E_a + E_k)^2 (E_a + E_l)} + \frac{2}{(E_a + E_k)(E_b + E_l)(E_a + E_b)} \right. \\
& + \frac{1}{(E_b + E_k)^2 (E_b + E_l)} + \frac{1}{(E_a + E_k)^2 (E_k + E_l)} + \frac{1}{(E_b + E_k)^2 (E_k + E_l)} \\
& + \frac{1}{(E_a + E_k)(E_a + E_l)(E_a + E_b)} + \frac{1}{(E_b + E_k)(E_b + E_l)(E_a + E_b)} \\
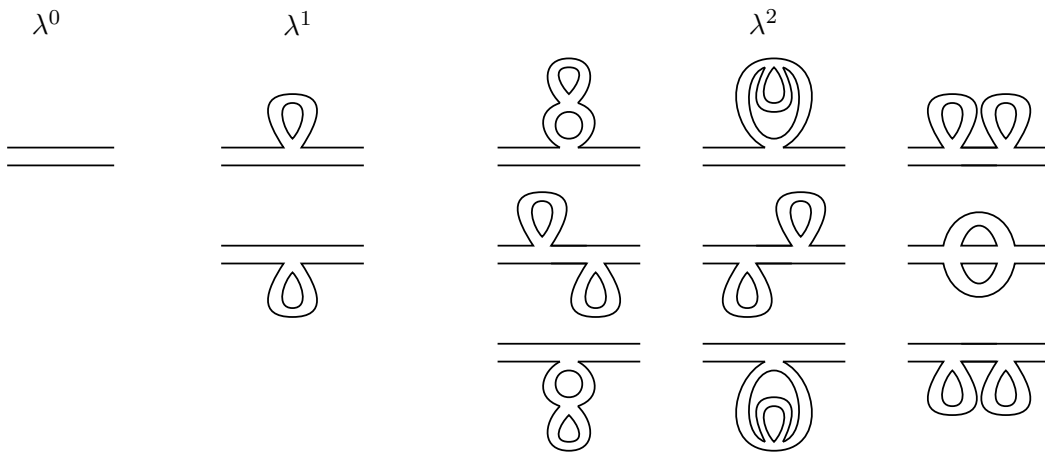& \left. + \frac{1}{(E_a + E_k)(E_b + E_l)(E_k + E_l)} \right) + \mathcal{O}(\lambda^3).
\end{aligned}
$$

Figure 3. All graphs contributing to the 2-point function $G_{|ab|}^{(0)}$ up to order λ^2, where the upper strand is labelled by a and the lower by b for each graph. Topologically, some graphs are the same but different elements of $\mathfrak{G}_{|ab|}^{0,v}$ due to different labellings.

Example 3.6. The second example will be the 4-point function to which 11 graphs contribute up to order λ^2 (see Figure 4). Taking the weights into account, we have perturbatively

$$
G^{(0)}_{|abcd|} = \frac{(-\lambda)}{(E_a+E_b)(E_b+E_c)(E_c+E_d)(E_d+E_a)} + \frac{(-\lambda)^2}{(E_a+E_b)(E_b+E_c)(E_c+E_d)(E_d+E_a)}
$$

$$
\times \frac{1}{N} \sum_{k=1}^{N} \Big(\frac{1}{(E_a+E_k)(E_a+E_b)} + \frac{1}{(E_a+E_k)(E_a+E_d)} + \frac{1}{(E_b+E_k)(E_b+E_c)}
$$

$$
+ \frac{1}{(E_b+E_k)(E_b+E_a)} + \frac{1}{(E_c+E_k)(E_c+E_d)} + \frac{1}{(E_c+E_k)(E_c+E_b)}
$$

$$
+ \frac{1}{(E_d+E_k)(E_d+E_a)} + \frac{1}{(E_d+E_k)(E_d+E_c)} + \frac{1}{(E_b+E_k)(E_d+E_k)}
$$

$$
+ \frac{1}{(E_a+E_k)(E_c+E_k)} \Big) + \mathcal{O}(\lambda^3).
$$
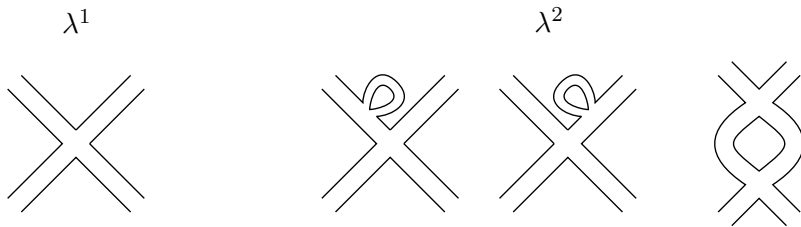
Figure 4. All graphs contributing to the 4-point function $G^{(0)}_{|abcd|}$ up to order λ^2, where the first two graphs of order λ^2 contribute with 4 different labellings and the last graph with 2 different labellings. In total this gives 10 different labelled ribbon graphs which contribute at order λ^2. These 11 labelled graphs are elements of $\mathfrak{G}^{0,v}_{|abcd|}$.

Example 3.7. The third example will be the $(2+2)$-point function to which 2 unlabelled ribbon graphs contribute up to order λ^2 (see Figure 5). Taking the weights into account, these split into 6 labelled ribbon graphs, leading to a perturbative expansion

$$
G^{(0)}_{|ab|cd|} = \frac{(-\lambda)^2}{(E_a + E_b)^2(E_c + E_d)^2} \Big(\frac{1}{(E_a + E_c)^2} + \frac{1}{(E_a + E_d)^2} + \frac{1}{(E_b + E_c)^2} + \frac{1}{(E_b + E_d)^2}
$$

$$
+ \frac{1}{(E_a + E_c)(E_b + E_d)} + \frac{1}{(E_a + E_d)(E_b + E_c)} \Big) + \mathcal{O}(\lambda^3).
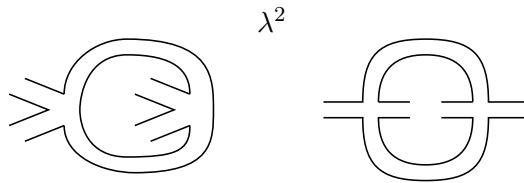$$

Figure 5. All graphs contributing to the $(2+2)$-point function $G^{(0)}_{|ab|cd|}$ up to order λ^2, where the left graph contributes with 4 different versions for the labelling and the right graph with 2 different versions for the labelling of the strands. This means that $\mathfrak{G}^{0,2}_{|ab|cd|}$ consists of 6 elements.

It is clear from the Feynman rules of Proposition 3.1 that at each order the correlation functions are rational functions of $E_{p_i^j}$ and E_{k_i}. Consequently the limit to coinciding indices $p_i^j \to p_{i'}^{j'}$ is well-defined at any order in λ.

For any $n_i > 2$, recursive algebraic relations between correlation functions are known; we refer to [25] for the general formula. In case of $(g, b) = (0, 1)$, the algebraic relation for the n_1-point function of genus zero is

$$G^{(0)}_{|p_1 p_2 \cdots p_{n_1}|} = -\lambda \sum_{k=1}^{\frac{n_1-2}{2}} \frac{G^{(0)}_{|p_{2k+2} \cdots p_{n_1} p_1|} G^{(0)}_{|p_2 \cdots p_{2k+1}|} - G^{(0)}_{|p_{2k+1} \cdots p_{n_1}|} G^{(0)}_{|p_1 \cdots p_{2k}|}}{(E_{p_{2k+1}} - E_{p_1})(E_{p_2} - E_{p_{n_1}})}.$$

The explicit combinatorial structure of this recursive equation was understood in [16] in form of two nested combinatorial problems each governed by Catalan numbers.

Example 3.8. The 4-point function is algebraically expressed in terms of the 2-point function by

$$G^{(0)}_{|abcd|} = -\lambda \frac{G^{(0)}_{|ad|} G^{(0)}_{|bc|} - G^{(0)}_{|ab|} G^{(0)}_{|cd|}}{(E_c - E_a)(E_b - E_d)}.$$

The reader can check that this equation holds at the first two orders by inserting Example 3.5 into the r.h.s. to recover Example 3.6.

4 Auxiliary functions of topological significance

4.1 Creation operator

The derivative

$$\hat{T}_q := -N \frac{\partial}{\partial E_q}$$

with respect to the parameters of the free theory, which we call *boundary creation operator*, plays a central rôle in [10]. It is used to define the auxiliary functions

$$T_{q_1,q_2,\ldots,q_m \| p_1^1 \cdots p_{n_1}^1 | p_1^2 \cdots p_{n_2}^2 | \cdots | p_1^b \cdots p_{n_b}^b |} := \hat{T}_{q_1} \cdots \hat{T}_{q_m} G_{|p_1^1 \cdots p_{n_1}^1 | p_1^2 \cdots p_{n_2}^2 | \cdots | p_1^b \cdots p_{n_b}^b |}$$

$$\Omega_{q_1,\ldots,q_m} := \hat{T}_{q_2} \cdots \hat{T}_{q_m} \Omega_{q_1} + \frac{\delta_{m,2}}{(E_{q_1} - E_{q_2})^2}, \qquad m \geq 2, \tag{4.1}$$

where

$$\Omega_q := \frac{1}{N} \sum_{k=1}^{N} G_{|qk|} + \frac{1}{N^2} G_{|q|q|}.$$

To define these functions properly it is necessary that all q_i, p_i^j are pairwise different. As before we introduce genus expansions $T_{q_1,q_2,\ldots,q_m \| p_1^1 \cdots p_{n_1}^1 | \cdots | p_1^b \cdots p_{n_b}^b |} = \sum_{g=0}^{\infty} N^{-2g} T^{(g)}_{q_1,q_2,\ldots,q_m \| p_1^1 \cdots p_{n_1}^1 | \cdots | p_1^b \cdots p_{n_b}^b |}$ and $\Omega_{q_1,\ldots,q_m} = \sum_{g=0}^{\infty} N^{-2g} \Omega^{(g)}_{q_1,\ldots,q_m}$.

Definition 4.1. The free energy $\mathcal{F}$ is defined to be a primitive of Ω_q under the creation operator, i.e., $\Omega_q^{(g)} =: \hat{T}_q \mathcal{F}^{(g)}$.

Main tool to evaluate applications of $\hat{T}_q$ is the equation of motion [32, Lemma 2] which can be reformulated as

$$\frac{1}{N} \frac{\partial \log \mathcal{Z}(M)}{\partial E_q} = \sum_{k=1}^{N} \left(\frac{\partial^2 \log \mathcal{Z}(M)}{\partial M_{qk} \partial M_{kq}} + \frac{\partial \log \mathcal{Z}(M)}{\partial M_{qk}} \frac{\partial \log \mathcal{Z}(M)}{\partial M_{kq}} \right)$$

$$+ \frac{1}{N} \sum_{k=1}^{N} G_{|qk|} + \frac{1}{N^2} G_{|q|q|}. \tag{4.2}$$

The following proposition gives the exact result for a single $\hat{T}_q$-operation. In its proof the assumption that the p_i^j are pairwise different and different from q is essential. For application of another $\hat{T}_{q'}$ on the result such an assumption does not hold. The calculation of several $\hat{T}$-operations must be carefully repeated.

Proposition 4.2. *For* $\mathcal{J} = p_1^1 \cdots p_{n_1}^1 | p_1^2 \cdots p_{n_2}^2 | \cdots | p_1^b \cdots p_{n_b}^b \equiv \left\{ J^1, \ldots, J^b \right\}$ *and* $J^i = [p_1^i, \ldots, p_{n_i}^i]$ *with all* p_l^j *pairwise different and different from* q *one has*

$$
\hat{T}_q G_{|\mathcal{J}|}^{(g)} = \frac{1}{N} \sum_{k=1}^N G_{|\mathcal{J}|qk|}^{(g)} + G_{|\mathcal{J}|q|q|}^{(g-1)} + \sum_{j=1}^b \sum_{l=1}^{n_j} G_{|[q,p_l^j] \triangleright_l J^j | \mathcal{J} \backslash J^j |}^{(g)} + \sum_{\substack{g_1+g_2=g \\ \mathcal{J}_1 \uplus \mathcal{J}_2 = \mathcal{J}}} G_{|\mathcal{J}_1|q|}^{(g_1)} G_{|\mathcal{J}_2|q|}^{(g_2)},
$$

where $[p_1, p_2, \ldots, p_i] \triangleright_l [q_1, q_2, \ldots, q_j] := [q_1, \ldots, q_l, p_1, \ldots, p_i, q_{l+1}, \ldots, q_j]$ *denotes the insertion of the first tuple after the* l^{th} *position of the second tuple,* $l = 0, \ldots, j$.

Proof. As in [10] we introduce derivative operators $\frac{D^{|\mathcal{J}|}}{DM^{\mathcal{J}}} = \frac{D^{|J^1|}}{DM^{J^1}} \cdots \frac{D^{|J^b|}}{D^{J^b}}$ with $\frac{D^n}{DM^{[p_1,\ldots,p_n]}} :=$ $\frac{(-iN)^n \partial^n}{\partial M_{p_1 p_2} \cdots \partial M_{p_{n-1} p_n} \partial M_{p_n p_1}}$. This gives a representation $G_{|\mathcal{J}|} = N^{b-2} \frac{D^{|\mathcal{J}|}}{DM^{\mathcal{J}}} \log \mathcal{Z}(M) \big|_{M=0}$ to which we apply $\hat{T}_q$ via (4.2):

$$
\hat{T}_q G_{|\mathcal{J}|} = N^{b-2} \sum_{k=1}^N \frac{D^{|\mathcal{J}|}}{DM^{\mathcal{J}}} \left(-N^2 \frac{\partial^2 \log \mathcal{Z}(M)}{\partial M_{qk} \partial M_{kq}} - N^2 \frac{\partial \log \mathcal{Z}(M)}{\partial M_{qk}} \frac{\partial \log \mathcal{Z}(M)}{\partial M_{kq}} \right) \Bigg|_{M=0}
$$

$$
= \frac{1}{N} \sum_{k=1}^N G_{|\mathcal{J}|qk|} + \frac{1}{N^2} G_{|\mathcal{J}|q|q|} + \sum_{j=1}^b \sum_{l=1}^{n_j} G_{|[q,p_l^j] \triangleright_l J^j | \mathcal{J} \backslash J^j |} + \sum_{\mathcal{J}_1 \uplus \mathcal{J}_2 = \mathcal{J}} G_{|\mathcal{J}_1|q|} G_{|\mathcal{J}_2|q|}.
$$

The second line results from the first line by the following considerations. The first term $N^{b-2} \frac{D^{|\mathcal{J}|}}{DM^{\mathcal{J}}} \frac{D^2(\log \mathcal{Z}(M))}{DM^{[q,k]}}$ contributes in three different ways:

(a) For generic k it produces $\frac{1}{N} G_{|\mathcal{J}|qk|}$.

(b) For $k = q$ it produces, besides $\frac{1}{N} G_{|\mathcal{J}|qq|}$ included in (a), also $\frac{1}{N^2} G_{|\mathcal{J}|q|q|}$ when interpreting $\frac{D^2}{DM^{[q,q]}} = \frac{D}{DM^{[q]}} \frac{D}{DM^{[q]}}$.

(c) For $k = p_l^j$ it produces, besides $\frac{1}{N} G_{|\mathcal{J}|qp_l^j|}$ included in (a), also $G_{|[q,p_l^j] \triangleright_l J^j | \mathcal{J} \backslash J^j |}$ when taking $\frac{D^{n^j}}{DM^{[p_1^j, \ldots, p_{n_j}^j]}} \frac{D^2}{DM^{[q,p_l^j]}} = \frac{D^{n_j+2}}{DM^{[p_1^j, \ldots, p_l^j, q, p_l^j, p_{l+1}^j, p_{n_j}^j]}}$ into account.

The second term of the first line only contributes for $k = q$ and for partitions of $\frac{D^{|\mathcal{J}|}}{DM^{\mathcal{J}}}$ into two blocks $\mathcal{J} = \mathcal{J}' \uplus \mathcal{J}''$ which preserve the J^j individually. Indeed, any splitting of the $\frac{D^n}{DM^{[p_1,\ldots,p_n]}}$ applied to $\mathcal{Z}(M)$ gives zero when setting $M = 0$.

Inserting $G_{\ldots} = \sum_{g=0}^\infty N^{-2g} G_{\ldots}^{(g)}$ in the second line and extracting the coefficient of N^{-2g} gives the assertion. ∎

Example 4.3. The action of the creation operator on the 2-point function reads

$$
\hat{T}_q G_{|p_1 p_2|}^{(g)} = \frac{1}{N} \sum_{k=1}^N G_{|p_1 p_2|qk|}^{(g)} + G_{|p_1 p_2|q|q|}^{(g-1)} + G_{|p_1 q p_1 p_2|}^{(g)} + G_{|p_1 p_2 q p_2|}^{(g)}.
$$

Example 4.4. The action of the creation operator on the $(1+1)$-point function reads

$$
\hat{T}_q G_{|p^1|p^2|}^{(g)} = \frac{1}{N} \sum_{k=1}^N G_{|p^1|p^2|qk|}^{(g)} + G_{|p^1|p^2|q|q|}^{(g-1)} + G_{|p^1 q p^1 | p^2|}^{(g)} + G_{|p^1 | p^2 q p^2|}^{(g)} + \sum_{g_1+g_2=g} G_{|p^1|q|}^{(g_1)} G_{|p^2|q|}^{(g_2)}.
$$

We also give a perturbative proof of Proposition 4.2. The creation operator $\hat{T}_q$ takes the derivative with respect to E_q of a rational function arising from the Feynman rules in Proposition 3.1. Since all external indices p_i^j are by assumption different from q, the derivative hits only the sums of the internal strands (loops) if the summation index coincides with q. Being a derivative, it is the sum over all strands of all internal loops. Isolating every such target as

$$\frac{1}{N} \sum_{k=1}^{N} \frac{1}{E_k + E_m} f(E_k, E_m, \dots),$$

where $f(E_k, E_m, \dots)$ is a rational function in E_k, E_m and further E_j, then the creation operator generates

$$\hat{T}_q \frac{1}{N} \sum_{k=1}^{N} \frac{1}{E_k + E_m} f(E_k, E_m, \dots) \to \frac{1}{(E_q + E_m)^2} f(E_q, E_m, \dots).$$

Graphically, a ribbon with internal strand labelled by k is hit by the creation operator $\hat{T}_q$. Its ribbon is cut into two ribbons each with weight $\frac{1}{E_q + E_m}$, where the previous loop label k is now fixed to q. Depending on the type of the other index m and the topology of the graph, four classes of ribbon graphs can be produced by action of $\hat{T}_q$:

1. The creation operator $\hat{T}_q$ acts on a ribbon in which both strands are internal strands, but different from each other. This means that m above is another summation index to which a summation operator $\frac{1}{N} \sum_{m=1}^{N}$ is assigned. The ribbon graph resulting from application of $\hat{T}_q$ thus receives an additional boundary component with 2 one-valent vertices with one strand fixed to q and the other to m with a summation over m. All other boundary components of the previous ribbon graphs are untouched. The resulting graph contributes to $\frac{1}{N} \sum_{m=1}^{N} G^{(g)}_{|p_1^1 \cdots p_{n_1}^1| \cdots |p_1^b \cdots p_{n_b}^b|qm|}$.
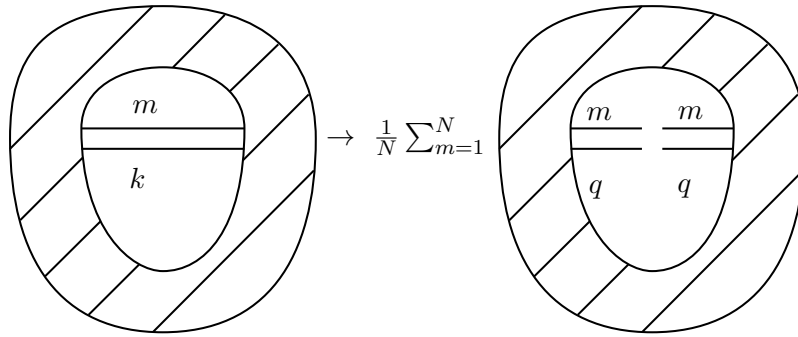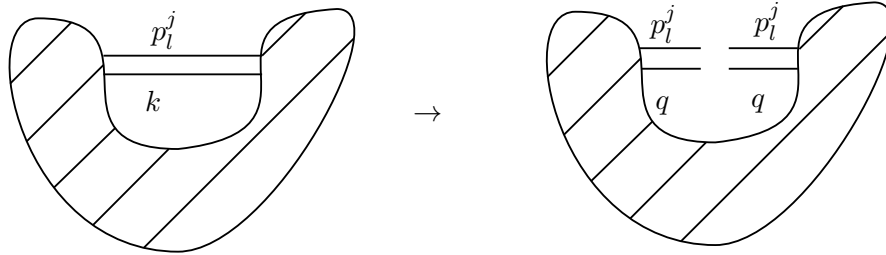

2. The creation operator $\hat{T}_q$ acts on a ribbon, where both strands are internal strands and the same, i.e., the index m is also set to k. Here we consider the case that after cutting the ribbon, the ribbon graph is still connected. Cutting the selected ribbon then decreases the genus by 1; otherwise it is not possible that both strands have the same label. Acting with $\hat{T}_q$ on the other strand of the same ribbon leads to the same result, thus a total factor of 2. The resulting graph has two additional boundary components each with 1 one-valent vertex with strands fixed to q. All other boundary components of the previous ribbon graphs are untouched. The resulting graph with its factor of 2 contributes to $G^{(g-1)}_{|p_1^1 \cdots p_{n_1}^1| \cdots |p_1^b \cdots p_{n_b}^b|q|q|}$. The factor of 2 accounts for the difference between labelled and unlabelled ribbon graphs. To see this consider $G^{(g-1)}_{|p_1^1 \cdots p_{n_1}^1| \cdots |p_1^b \cdots p_{n_b}^b|q'|q''|}$ with $q' \neq q''$ in which

every topological ribbon graph occurs twice, namely first with labels q', q'' on an ordered pair of open lines and second with labels q'', q' on that pair. When setting $q' = q'' = q$ we get twice the same labelled ribbon graph.
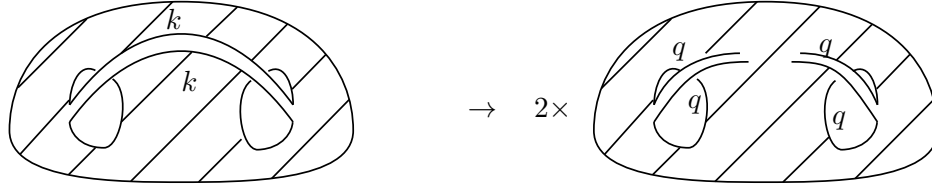
3. The creation operator $\hat{T}_q$ acts on a ribbon, where one strand is internal and the other external, i.e., the index m above is some p_l^j. After cutting the ribbon, the previously internal strand becomes part of the jth boundary component. The resulting ribbon graph receives 2 additional one-valent vertices next to each other, with attached ribbons labelled $p_l^j q$ and $q p_l^j$, at the jth boundary component. All other $b-1$ boundary components are untouched. The resulting ribbon graph thus contributes to $G^{(g)}_{|p_1^1 \cdots p_{n_1}^1| p_1^j \cdots p_{l-1}^j p_l^j q p_l^j p_{l+1}^j \cdots p_{n_j}^j| p_1^b \cdots p_{n_b}^b|}$.

4. The creation operator $\hat{T}_q$ acts on a ribbon, where both strands are internal strands of the same label k, but in contrast to Case 2 the ribbon graph disconnects after cutting the ribbon. Acting with $\hat{T}_q$ on the other strand also labelled k gives the same splitting, thus a total factor of 2. Each of the two resulting connected ribbon graphs receives an additional boundary component with a single one-valent vertex whose ribbon is labelled qq. All previous boundaries with labels $\mathcal{J}$ as well as the total genus g are untouched, but split into each of the ribbon graphs. This splitting accounts for the additional factor of 2 because for given assignment $\mathcal{J}'$, $\mathcal{J}''$ the decompositions $\mathcal{J}' \uplus \mathcal{J}'' = \mathcal{J}$ and $\mathcal{J}'' \uplus \mathcal{J}' = \mathcal{J}$ are considered as different. The resulting ribbon graph thus contributes to $G^{(g_1)}_{|\mathcal{J}_1|q|} G^{(g_2)}_{|\mathcal{J}_2|q|}$ with sum over $g_1 + g_2 = g$ and over splittings $\mathcal{J}_1 \uplus \mathcal{J}_2 = \mathcal{J}$.
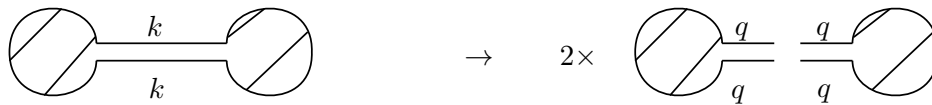
Notice that for the vacuum ribbon graphs of the free energy $\mathcal{F}^{(g)}$ only the two Cases 1 and 2 contribute. Case 3 contributes only if a ribbon graph has an external strand, which is not the case for a vacuum ribbon graph, and Case 4 does not contribute because any vacuum ribbon graph is a 1PI (one particle irreducible) due to four-valent vertices, i.e., after cutting a ribbon the graph stays connected.

Example 4.5. Take Example 4.3 for $g = 0$ with its ribbon graph expansion. The first orders of the expansion of the 2-point function are given in Example 3.5 with ribbon graphs drawn in Figure 3. The perturbative action of the creation operator described above generates the

corresponding contributions of the 4-point function and the $(2+2)$-point function, which can be taken from the Examples 3.6 and 3.7, where the graphs are drawn in Figures 4 and 5. It is left to the reader to check the explicit formulae.

Example 4.6. The action of the creation operator on the free energy of genus $g = 0$ is

$$\hat{T}_q \mathcal{F}^{(0)} = \frac{1}{N} \sum_{k=1}^{N} G_{|qk|}^{(0)}.$$

Take the perturbative expansion of the free energy from Example 3.4 with ribbon graphs drawn in Figure 2. The symmetry factor of the automorphism group of each ribbon graph ensures that the ribbon graphs generated by the creation operator have correct factors in agreement with Example 3.5. Consequently, this gives a way to compute the order of the automorphism group. For instance, the contribution of the sunrise graph to $\frac{1}{N} \sum_{k=1}^{N} G_{|qk|}^{(0)}$ is generated in 8 different ways by acting with the creation operator at the melon graph Γ_M of $\mathcal{F}^{(0)}$, which hence has $|\text{Aut}(\Gamma_M)| = 8$.

We conclude that the action of the creation operator can be represented in two different but equivalent ways, first directly on the correlation functions by using manipulations of the partition function and second perturbatively by using the action on the weighted graphs.

4.2 Representation of $\Omega^{(g)}$ in terms of correlation functions

We have shown in [10] that the $\Omega_{q_1,\ldots,q_m}^{(g)}$ defined in (4.1) extend to meromorphic differential forms $\omega_{g,m}$ on $\hat{\mathbb{C}}^m$ for which we provided strong evidence [5] and a proof for $g = 0$ [26] that they obey blobbed topological recursion. If true the $\omega_{g,m}$ are relatively easy to obtain via evaluation of residues. The translation back to $\Omega_{q_1,\ldots,q_m}^{(g)}$ is simple. In this section we give another representation of the $\Omega_{q_1,\ldots,q_m}^{(g)}$ as special polynomials in the correlation functions $G_{\cdots}^{(g')}$. The purpose is twofold. First, comparison of a perturbative expansion of the $G_{\cdots}^{(g')}$ with a Taylor expansion of the exact formulae provides an important consistency check. Second, we understand our observation as a message for quantum field theory in general: Also in realistic QFT it might be worthwhile to investigate whether certain polynomials of correlation functions, which themselves are Feynman graph series, reveal a deeper structure than individual functions or graphs.

The definition already gives $\Omega_{q_1}^{(g)} = \frac{1}{N} \sum_{k=1}^{N} G_{|q_1k|}^{(g)} + G_{|q_1q_1|}^{(g-1)}$. The next two propositions provide $\Omega_{q_1,q_2}^{(g)}$ and $\Omega_{q_1,q_2,q_3}^{(g)}$. It would be straightforward but increasingly lengthy to continue.

Proposition 4.7. *For $q_1 \neq q_2$ one has*

$$\Omega_{q_1,q_2}^{(g)} = \frac{\delta_{g,0}}{(E_{q_1} - E_{q_2})^2} + \sum_{g_1+g_2=g} G_{|q_1q_2|}^{(g_1)} G_{|q_1q_2|}^{(g_2)} + \frac{1}{N^2} \sum_{k,l=1}^{N} G_{|q_1k|q_2l|}^{(g)}$$

$$+ \frac{1}{N} \sum_{k=1}^{N} \left(G_{|q_1kq_1q_2|}^{(g)} + G_{|q_2kq_2q_1|}^{(g)} + G_{|q_1kq_2k|}^{(g)} \right) + \frac{1}{N} \sum_{k=1}^{N} \left(G_{|q_1k|q_2|q_2|}^{(g-1)} + G_{|q_2k|q_1|q_1|}^{(g-1)} \right)$$

$$+ G_{|q_1q_2q_2|q_2|}^{(g-1)} + G_{|q_2q_1q_1|q_1|}^{(g-1)} + \sum_{g_1+g_2=g-1} G_{|q_1q_2|}^{(g_1)} G_{|q_1q_2|}^{(g_2)} + G_{|q_1q_1|q_2q_2|}^{(g-2)}.$$

Proof. Using $\Omega_{q_1} = \frac{1}{N^2} \sum_{k=1}^{N} \frac{D^2}{DM^{[q_1,k]}} \log \mathcal{Z}(M)\big|_{M=0}$ and (4.2) we have

$$\hat{T}_{q_2} \Omega_{q_1} = -\sum_{k,l=1}^{N} \frac{D^2}{DM^{[q_1,k]}} \left(\frac{\partial^2 \log \mathcal{Z}(M)}{\partial M_{q_2l} \partial M_{lq_2}} + \frac{\partial \log \mathcal{Z}(M)}{\partial M_{q_2l}} \frac{\partial \log \mathcal{Z}(M)}{\partial M_{lq_2}} \right)\bigg|_{M=0}$$

$$= \frac{1}{N^2} \sum_{k,l=1}^{N} G_{|q_1 k|q_2 l|} + \frac{1}{N} \sum_{k=1}^{N} \left(G_{|q_1 k q_1 q_2|} + G_{|q_2 k q_2 q_1|} + G_{|q_1 k q_2 k|} \right) + G_{|q_1 q_2|} G_{|q_1 q_2|}$$

$$+ \frac{1}{N^3} \sum_{k=1}^{N} \left(G_{|q_1 k|q_2 q_2|} + G_{|q_2 k|q_1 q_1|} \right) + \frac{1}{N^2} \left(G_{|q_1 q_2 q_2|q_2|} + G_{|q_2 q_1 q_1|q_1|} \right)$$

$$+ \frac{1}{N^2} G_{|q_1|q_2|} G_{|q_1|q_2|} + \frac{1}{N^4} G_{|q_1 q_1|q_2 q_2|}. \tag{4.3}$$

The last three lines result from the first line of (4.3) as follows. The first term $\frac{1}{N^2} \frac{D^2}{DM^{[q_1,k]}} \times \frac{D^2(\log \mathcal{Z}(M))}{DM^{[q_2,l]}}$ contributes in nine different ways:

(a) For generic k, l it produces $\frac{1}{N^2} G_{|q_1 k|q_2 l|}$ summed over k, l.

(b) For $l = q_1$ it produces, besides $\frac{1}{N^2} G_{|q_1 k|q_2 q_1|}$ included in (a), also $\frac{1}{N} G_{|q_1 k q_1 q_2|}$ when interpreting $\frac{D^2}{DM^{[q_1,k]}} \frac{D^2}{DM^{[q_2,q_1]}} = \frac{D^4}{DM^{[q_1,k,q_1,q_2]}}$.

(c) For $k = q_2$ it produces, besides $\frac{1}{N^2} G_{|q_1 q_2|q_2 l|}$ included in (a), also $\frac{1}{N} G_{|q_2 l q_2 q_1|}$ when interpreting $\frac{D^2}{DM^{[q_1,q_2]}} \frac{D^2}{DM^{[q_2,l]}} = \frac{D^4}{DM^{[q_2,l,q_2,q_1]}}$. We replace $l \mapsto k$.

(d) For $l = k$ it produces, besides $\frac{1}{N^2} G_{|q_1 k|q_2 k|}$ included in (a), also $\frac{1}{N} G_{|q_1 k q_2 k|}$ when interpreting $\frac{D^2}{DM^{[q_1,k]}} \frac{D^2}{DM^{[q_2,k]}} = \frac{D^4}{DM^{[q_1,k,q_2,k]}}$.

(e) For $l = q_2$ it produces, besides $\frac{1}{N^2} G_{|q_1 k|q_2 q_2|}$ included in (a), also $\frac{1}{N^3} G_{|q_1 k|q_2 q_2|}$ when interpreting $\frac{D^2}{DM^{[q_1,k]}} \frac{D^2}{DM^{[q_2,q_2]}} = \frac{D^2}{DM^{[q_1,k]}} \frac{D^1}{DM^{[q_2]}} \frac{D^1}{DM^{[q_2]}}$.

(f) For $k = q_1$ it produces, besides $\frac{1}{N^2} G_{|q_1 q_1|q_2 l|}$ included in (a), also $\frac{1}{N^3} G_{|q_2 l|q_1 q_1|}$ when interpreting $\frac{D^2}{DM^{[q_1,q_1]}} \frac{D^2}{DM^{[q_2,l]}} = \frac{D^2}{DM^{[q_2,l]}} \frac{D^1}{DM^{[q_1]}} \frac{D^1}{DM^{[q_1]}}$. We replace $l \mapsto k$.

(g) For $k = l = q_2$ it produces, besides the three cases $\frac{1}{N^2} G_{|q_1 q_2|q_2 q_2|}$ included in (a), $\frac{1}{N} G_{|q_2 q_2 q_2 q_1|}$ included in (c) and $\frac{1}{N^3} G_{|q_1 q_2|q_2 q_2|}$ included in (e), also $\frac{1}{N^2} G_{|q_1 q_2 q_2|q_2|}$ when interpreting $\frac{D^2}{DM^{[q_1,q_2]}} \frac{D^2}{DM^{[q_2,q_2]}} = \frac{D^3}{DM^{[q_1,q_2,q_2]}} \frac{D^1}{DM^{[q_2]}}$.

(h) For $k = l = q_1$ it produces, besides the three cases $\frac{1}{N^2} G_{|q_1 q_1|q_2 q_1|}$ included in (a), $\frac{1}{N} G_{|q_1 q_1 q_1 q_2|}$ included in (b) and $\frac{1}{N^3} G_{|q_2 q_1|q_1 q_1|}$ included in (f), also $\frac{1}{N^2} G_{|q_2 q_1 q_1|q_1|}$ when interpreting $\frac{D^2}{DM^{[q_1,q_1]}} \frac{D^2}{DM^{[q_2,q_1]}} = \frac{D^3}{DM^{[q_2,q_1,q_1]}} \frac{D^1}{DM^{[q_1]}}$.

(i) For $k = q_1$ and $l = q_2$ it produces, besides the three cases $\frac{1}{N^2} G_{|q_1 q_1|q_2 q_2|}$ included in (a), $\frac{1}{N^3} G_{|q_1 q_1|q_2 q_2|}$ included in (e) and $\frac{1}{N^3} G_{|q_1 q_1|q_2 q_2|}$ included in (f), also $\frac{1}{N^4} G_{|q_1 q_1|q_2 q_2|}$ when interpreting $\frac{D^2}{DM^{[q_1,q_1]}} \frac{D^2}{DM^{[q_2,q_2]}} = \frac{D^1}{DM^{[q_1]}} \frac{D^1}{DM^{[q_1]}} \frac{D^1}{DM^{[q_2]}} \frac{D^1}{DM^{[q_2]}}$.

The second term $-\frac{1}{N^2} \frac{D^2}{DM^{[q_1,k]}} \frac{\partial \log \mathcal{Z}(M)}{\partial M_{q_2 l}} \frac{\partial \log \mathcal{Z}(M)}{\partial M_{l q_2}}$ contributes in two different ways:

(a) Either $k = q_2$ and $l = q_1$ and derivatives distributed into $\frac{1}{N^2} \frac{D^2 \log \mathcal{Z}(M)}{DM^{[q_1,q_2]}} \frac{D^2 \log \mathcal{Z}(M)}{DM^{[q_1,q_2]}} = G_{|q_1 q_2|} G_{|q_1 q_2|}$,

(b) or $k = q_1$ and $l = q_2$ and derivatives distributed into $\frac{1}{N^2} \frac{D^2 \log \mathcal{Z}(M)}{DM^{[q_1]} DM^{[q_2]}} \frac{D^2 \log \mathcal{Z}(M)}{DM^{[q_1]} DM^{[q_2]}} = \frac{1}{N^2} G_{|q_1|q_2|} G_{|q_1|q_2|}$.

Including the special term $\frac{1}{(E_{q_1} - E_{q_2})^2}$ and extracting the coefficient of N^{-2g} gives the assertion. ∎

Proposition 4.8. *For pairwise different q_1, q_2, q_3 one has*

$$
\begin{aligned}
\Omega_{q_1,q_2,q_3}^{(g)} = {} & \frac{1}{N^3} \sum_{j,k,l=1}^{N} G_{|q_1 j|q_2 k|q_3 l|}^{(g)} \\
& + \frac{1}{N^2} \sum_{k,l=1}^{N} \Big(G_{|q_1 k q_2 k|q_3 l|}^{(g)} + G_{|q_2 k q_3 k|q_1 l|}^{(g)} + G_{|q_3 k q_1 k|q_2 l|}^{(g)} + G_{|q_1 k q_1 q_2|q_3 l|}^{(g)} \\
& \qquad + G_{|q_1 k q_1 q_3|q_2 l|}^{(g)} + G_{|q_2 k q_2 q_3|q_1 l|}^{(g)} + G_{|q_2 k q_2 q_1|q_3 l|}^{(g)} + G_{|q_3 k q_3 q_1|q_2 l|}^{(g)} + G_{|q_3 k q_3 q_2|q_1 l|}^{(g)} \Big) \\
& + \frac{1}{N} \sum_{k=1}^{N} \Big(G_{|q_1 k q_2 k q_3 k|}^{(g)} + G_{|q_1 k q_3 k q_2 k|}^{(g)} + G_{|q_1 k q_1 q_2 q_1 q_3|}^{(g)} + G_{|q_1 k q_1 q_3 q_1 q_2|}^{(g)} \\
& \qquad + G_{|q_2 k q_2 q_3 q_2 q_1|}^{(g)} + G_{|q_2 k q_2 q_1 q_2 q_3|}^{(g)} + G_{|q_3 k q_3 q_1 q_3 q_2|}^{(g)} + G_{|q_3 k q_3 q_2 q_3 q_1|}^{(g)} \\
& \qquad + G_{|q_1 k q_1 q_2 q_3 q_2|}^{(g)} + G_{|q_1 k q_1 q_3 q_2 q_3|}^{(g)} + G_{|q_2 k q_2 q_3 q_1 q_3|}^{(g)} + G_{|q_2 k q_2 q_1 q_3 q_1|}^{(g)} \\
& \qquad + G_{|q_3 k q_3 q_1 q_2 q_1|}^{(g)} + G_{|q_3 k q_3 q_2 q_1 q_2|}^{(g)} + G_{|k q_1 k q_2 q_3 q_2|}^{(g)} + G_{|k q_1 k q_3 q_2 q_3|}^{(g)} \\
& \qquad + G_{|k q_2 k q_3 q_1 q_3|}^{(g)} + G_{|k q_2 k q_1 q_3 q_1|}^{(g)} + G_{|k q_3 k q_1 q_2 q_1|}^{(g)} + G_{|k q_3 k q_2 q_1 q_2|}^{(g)} \Big) \\
& + 2 \sum_{g_1+g_2=g} \frac{1}{N} \sum_{k=1}^{N} \Big(G_{|q_1 q_2|}^{(g_1)} G_{|q_3 k|q_1 q_2|}^{(g_2)} + G_{|q_1 q_2|}^{(g_1)} G_{|q_1 q_2 q_1 q_3|}^{(g_2)} + G_{|q_1 q_2|}^{(g_1)} G_{|q_2 q_1 q_2 q_3|}^{(g_2)} \\
& \qquad + G_{|q_2 q_3|}^{(g_1)} G_{|q_1 k|q_2 q_3|}^{(g_2)} + G_{|q_2 q_3|}^{(g_1)} G_{|q_2 q_3 q_2 q_1|}^{(g_2)} + G_{|q_2 q_3|}^{(g_1)} G_{|q_3 q_2 q_3 q_1|}^{(g_2)} \\
& \qquad + G_{|q_3 q_1|}^{(g_1)} G_{|q_2 k|q_3 q_1|}^{(g_2)} + G_{|q_3 q_1|}^{(g_1)} G_{|q_3 q_1 q_3 q_2|}^{(g_2)} + G_{|q_3 q_1|}^{(g_1)} G_{|q_1 q_3 q_1 q_2|}^{(g_2)} \Big) \\
& + \frac{1}{N^2} \sum_{k,l=1}^{N} \Big(G_{|q_1 k|q_2 l|q_3|q_3|}^{(g-1)} + G_{|q_2 k|q_3 l|q_1|q_1|}^{(g-1)} + G_{|q_3 k|q_1 l|q_2|q_2|}^{(g-1)} \Big) \\
& + \frac{1}{N} \sum_{l=1}^{N} \Big(G_{|q_1 q_1 q_2|q_3 l|q_1|}^{(g-1)} + G_{|q_1 q_1 q_3|q_2 l|q_1|}^{(g-1)} + G_{|q_2 q_2 q_3|q_1 l|q_2|}^{(g-1)} + G_{|q_2 q_2 q_1|q_3 l|q_2|}^{(g-1)} \\
& \qquad + G_{|q_3 q_3 q_1|q_2 l|q_3|}^{(g-1)} + G_{|q_3 q_3 q_2|q_1 l|q_3|}^{(g-1)} \Big) \\
& + G_{|q_1 q_1 q_2 q_3 q_2|q_1|}^{(g-1)} + G_{|q_1 q_1 q_3 q_2 q_3|q_1|}^{(g-1)} + G_{|q_2 q_2 q_3 q_1 q_3|q_2|}^{(g-1)} + G_{|q_2 q_2 q_1 q_3 q_1|q_2|}^{(g-1)} \\
& + G_{|q_3 q_3 q_1 q_2 q_1|q_3|}^{(g-1)} + G_{|q_3 q_3 q_2 q_1 q_2|q_3|}^{(g-1)} + G_{|q_1 q_1 q_2 q_1 q_3|q_1|}^{(g-1)} + G_{|q_1 q_1 q_3 q_1 q_2|q_1|}^{(g-1)} \\
& + G_{|q_2 q_2 q_3 q_2 q_1|q_2|}^{(g-1)} + G_{|q_2 q_2 q_1 q_2 q_3|q_2|}^{(g-1)} + G_{|q_3 q_3 q_1 q_3 q_2|q_3|}^{(g-1)} + G_{|q_3 q_3 q_2 q_3 q_1|q_3|}^{(g-1)} \\
& + G_{|q_1 q_1 q_2|q_1 q_1 q_3|}^{(g-1)} + G_{|q_2 q_2 q_3|q_2 q_2 q_1|}^{(g-1)} + G_{|q_3 q_3 q_1|q_3 q_3 q_2|}^{(g-1)} \\
& + \frac{1}{N} \sum_{k=1}^{N} \Big(G_{|q_1 k q_2 k|q_3|q_3|}^{(g-1)} + G_{|q_2 k q_3 k|q_1|q_1|}^{(g-1)} + G_{|q_3 k q_1 k|q_2|q_2|}^{(g-1)} \\
& \qquad + G_{|q_1 k q_1 q_2|q_3|q_3|}^{(g-1)} + G_{|q_1 k q_1 q_3|q_2|q_2|}^{(g-1)} + G_{|q_2 k q_2 q_3|q_1|q_1|}^{(g-1)} + G_{|q_2 k q_2 q_1|q_3|q_3|}^{(g-1)} \\
& \qquad + G_{|q_3 k q_3 q_1|q_2|q_2|}^{(g-1)} + G_{|q_3 k q_3 q_2|q_1|q_1|}^{(g-1)} \Big) \\
& + 2 \sum_{g_1+g_2=g-1} \Big(G_{|q_1 q_2|}^{(g_1)} G_{|q_1 q_2|q_3|q_3|}^{(g_2)} + G_{|q_2 q_3|}^{(g_1)} G_{|q_2 q_3|q_1|q_1|}^{(g_2)} + G_{|q_3 q_1|}^{(g_1)} G_{|q_3 q_1|q_2|q_2|}^{(g_2)} \Big) \\
& + 4 \sum_{g_1+g_2=g-1} \frac{1}{N} \sum_{k=1}^{N} \Big(G_{|q_1 q_2|}^{(g_1)} G_{|q_3 k|q_1 q_2|}^{(g_2)} + G_{|q_2 q_3|}^{(g_1)} G_{|q_1 k|q_2 q_3|}^{(g_2)} + G_{|q_3 q_1|}^{(g_1)} G_{|q_2 k|q_3 q_1|}^{(g_2)} \Big)
\end{aligned}
$$

$$+ 4 \sum_{g_1+g_2=g-1} \left(G^{(g_1)}_{|q_1|q_2|} G^{(g_2)}_{|q_2|q_1q_1q_3|} + G^{(g_1)}_{|q_1|q_2|} G^{(g_2)}_{|q_1|q_2q_2q_3|} + G^{(g_1)}_{|q_2|q_3|} G^{(g_2)}_{|q_3|q_2q_2q_1|} \right.$$

$$\left. + G^{(g_1)}_{|q_2|q_3|} G^{(g_2)}_{|q_2|q_3q_3q_1|} + G^{(g_1)}_{|q_3|q_1|} G^{(g_2)}_{|q_1|q_3q_3q_2|} + G^{(g_1)}_{|q_3|q_1|} G^{(g_2)}_{|q_3|q_1q_1q_2|} \right)$$

$$+ 8 \sum_{g_1+g_2+g_3=g-1} G^{(g_1)}_{|q_1|q_2|} G^{(g_2)}_{|q_2|q_3|} G^{(g_3)}_{|q_3|q_1|} + G^{(g-2)}_{|q_1q_1q_2|q_3|q_3|q_1|} + G^{(g-2)}_{|q_1q_1q_3|q_2|q_2|q_1|}$$

$$+ G^{(g-2)}_{|q_2q_2q_3|q_1|q_1|q_2|} + G^{(g-2)}_{|q_2q_2q_1|q_3|q_3|q_2|} + G^{(g-2)}_{|q_3q_3q_1|q_2|q_2|q_3|} + G^{(g-2)}_{|q_3q_3q_2|q_1|q_1|q_3|}$$

$$+ \frac{1}{N} \sum_{k=1}^{N} \left(G^{(g-2)}_{|q_1k|q_2|q_2|q_3|q_3|} + G^{(g-2)}_{|q_2k|q_3|q_3|q_1|q_1|} + G^{(g-2)}_{|q_3k|q_1|q_1|q_2|q_2|} \right)$$

$$+ 4 \sum_{g_1+g_2=g-2} \left(G^{(g_1)}_{|q_1|q_2|} G^{(g_2)}_{|q_1|q_2|q_3|q_3|} + G^{(g_1)}_{|q_2|q_3|} G^{(g_2)}_{|q_2|q_3|q_1|q_1|} + G^{(g_1)}_{|q_3|q_1|} G^{(g_2)}_{|q_3|q_1|q_2|q_2|} \right)$$

$$+ G^{(g-3)}_{|q_1|q_1|q_2|q_2|q_3|q_3|}.$$

Proof. Applications of $\hat{T}_{q_3}$ to the first line of (4.3) gives with (4.2)

$$\hat{T}_{q_3} \hat{T}_{q_2} \Omega_{q_1} = N^2 \sum_{j,k,l=1}^{N} \frac{D^2}{DM^{[q_1,k]}} \left\{ \frac{\partial^2}{\partial M_{q_2l} \partial M_{lq_2}} \left(\frac{\partial^2 \log \mathcal{Z}(M)}{\partial M_{q_3j} \partial M_{jq_3}} + \frac{\partial \log \mathcal{Z}(M)}{\partial M_{q_3j}} \frac{\partial \log \mathcal{Z}(M)}{\partial M_{jq_3}} \right) \right.$$

$$+ \frac{\partial}{\partial M_{q_2l}} \left(\frac{\partial^2 \log \mathcal{Z}(M)}{\partial M_{q_3j} \partial M_{jq_3}} + \frac{\partial \log \mathcal{Z}(M)}{\partial M_{q_3j}} \frac{\partial \log \mathcal{Z}(M)}{\partial M_{jq_3}} \right) \frac{\partial \log \mathcal{Z}(M)}{\partial M_{lq_2}}$$

$$\left. + \frac{\partial}{\partial M_{lq_2}} \left(\frac{\partial^2 \log \mathcal{Z}(M)}{\partial M_{q_3j} \partial M_{jq_3}} + \frac{\partial \log \mathcal{Z}(M)}{\partial M_{q_3j}} \frac{\partial \log \mathcal{Z}(M)}{\partial M_{jq_3}} \right) \frac{\partial \log \mathcal{Z}(M)}{\partial M_{q_2l}} \right\} \Bigg|_{M=0}.$$

A similar discussion as before gives the assertion. ∎

Using the previous Examples 3.5, 3.6 and 3.7, it is easy to write $\Omega^{(0)}_{q_1}$ and $\Omega^{(0)}_{q_1,q_2}$ up to order λ^2 and $\Omega^{(0)}_{q_1,q_2,q_3}$ up to order λ^1.

5 Results connected with blobbed topological recursion

In the next subsection we briefly recall the main construction of [10] how *explicit and exact* results for $\Omega^{(g)}_{b_1,\dots,b_m}$ are obtained. Afterwards, the first few examples are expanded in λ and shown to reproduce the perturbative results.

5.1 Summary of previous work

Our main tool is the usage of *Dyson–Schwinger equations*. They are first derived for the correlation functions $G^{(g)}_{\dots}$ introduced before, then complexified to functions $G^{(g)}$ of several complex variables which satisfy $G^{(g)}\left(E_{p_1^1}, \dots, E_{p_{n_1}^1} | \cdots | E_{p_1^b}, \dots, E_{p_{n_b}^b}\right) = G^{(g)}_{|p_1^1\cdots p_{n_1}^1|\cdots|p_1^b\cdots p_{n_b}^b|}$. After complexification one can admit multiplicities of the E_k, i.e., we assume that $(e_1, \dots, e_d)$ are the pairwise different values in $(E_1, \dots, E_N)$ which arise with multiplicities $(r_1, \dots, r_d)$, respectively, with $r_1 + \cdots + r_d = N$. It is also straightforward to take a limit, where the e_k continuously fill an interval with a certain spectral measure. As mentioned before, there is a closed non-linear equation [23, 24] for the planar 2-point function alone and an infinite hierarchy of affine equations for all other functions. A continuum variant of the non-linear equation was solved in [31] for the 2-dimensional Moyal case and later in [21] in full generality. It suggested an ansatz in which an implicitly defined function $R: \hat{\mathbb{C}} \to \hat{\mathbb{C}}$, where $\hat{\mathbb{C}} = \mathbb{C} \cup \{\infty\}$, is crucial:

Theorem 5.1 ([32]). *Let $(E_1, \ldots, E_N)$ be partitioned into pairwise different $e_1, \ldots, e_d > 0$ which arise with multiplicities $(r_1, \ldots, r_d)$, respectively. Assume that the complexification $\hat{\Omega}^{(0)}(E_q) = \Omega_q^{(0)}$ can be expressed as*

$$\hat{\Omega}^{(0)}(R(z)) =: \Omega_1^{(0)}(z) = -\frac{R(-z) + R(z)}{\lambda} - \frac{1}{N} \sum_{k=1}^{d} \frac{r_k}{R(\varepsilon_k) - R(z)} \tag{5.1}$$

for some meromorphic function R of degee $d+1$ with $R(\varepsilon_k) = e_k$ and $R(\infty) = \infty$. Then R is, for generic values of (e_k), uniquely determined by the non-linear Dyson–Schwinger equation to

$$R(z) := z - \frac{\lambda}{N} \sum_{k=1}^{d} \frac{\varrho_k}{\varepsilon_k + z}, \qquad \varrho_k = \frac{r_k}{R'(\varepsilon_k)}. \tag{5.2}$$

Choosing $\lim_{\lambda \to 0} \varepsilon_k = e_k$, then any (e_k) is generic for λ in an open (real or complex) neighbourhood of 0.

The implicitly defined function R provides a ramified covering $R \colon \hat{\mathbb{C}} \to \hat{\mathbb{C}}$ of Riemann spheres, see Figure 6. The important observation is that R pulls $\hat{\Omega}^{(0)}(\zeta)$ back to a *rational* function $\Omega_1^{(0)}(z)$. This rationality on the (right) z-plane of Figure 6 extends to all other correlation functions. In contrast, when expressing these functions in terms of the original variables (e_k) we need to invert R which in closed form is not possible beside $d = 1$.
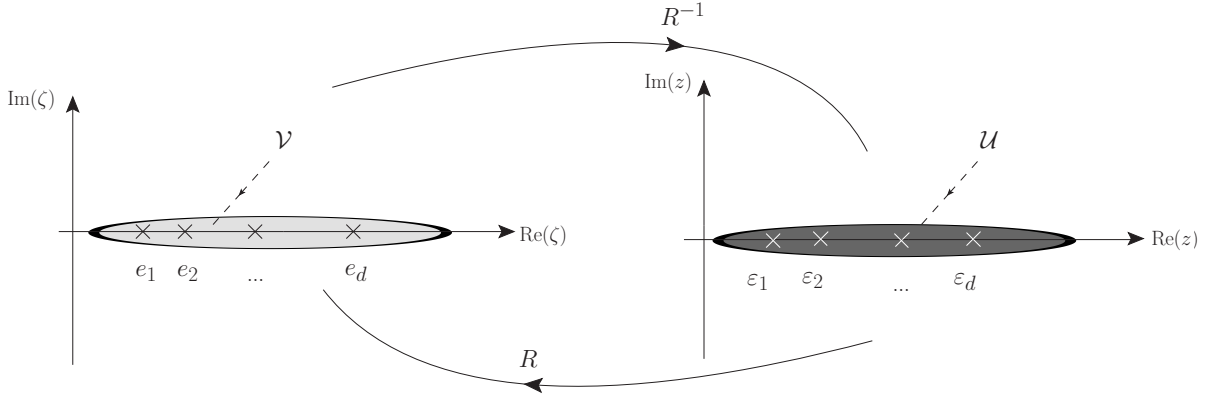

Figure 6. Illustration of the ramified covering map $R \colon \hat{\mathbb{C}} \to \hat{\mathbb{C}}$ satisfying $R(\varepsilon_k) = e_k$. The map R is biholomorphic between the neighbourhoods $\mathcal{V}$ and $\mathcal{U}$.

It was understood in [10] that, although all other complexified functions $G^{(g)}$ satisfy affine Dyson–Schwinger equations (see [25]), an explicit solution must first be achieved for the auxiliary functions $\Omega_m^{(g)}(z_1, \ldots, z_m)$ with $\Omega_m^{(g)}(\varepsilon_{q_1}, \ldots, \varepsilon_{q_m}) = \Omega_{q_1,\ldots,q_m}^{(g)}$. We refer to [10] for details about the solution strategy for $\Omega_m^{(g)}(z_1, \ldots, z_m)$. Here we only quote the remarkably simple result:

Proposition 5.2 ([10]). *Let $R(z)$ be as in Theorem 5.1 and β_i for $i \in \{1, \ldots, 2d\}$ be the $2d$ solutions of $R'(z) = 0$. We have the solutions*

$$\Omega_2^{(0)}(u, z) = \frac{1}{R'(u)R'(z)} \left(\frac{1}{(u-z)^2} + \frac{1}{(u+z)^2} \right),$$

$$\Omega_3^{(0)}(u, v, z) = \frac{1}{R'(u)R'(v)R'(z)} \frac{\partial^3}{\partial u \partial v \partial z} \left[\frac{\lambda\left(\frac{1}{v+u} + \frac{1}{v-u}\right)}{R'(u)R'(-u)(z+u)} + \frac{\lambda\left(\frac{1}{u+v} + \frac{1}{u-v}\right)}{R'(v)R'(-v)(z+v)} \right.$$

$$\left. + \sum_{i=1}^{2d} \frac{\lambda\left(\frac{1}{v+\beta_i} + \frac{1}{v-\beta_i}\right)\left(\frac{1}{u+\beta_i} + \frac{1}{u-\beta_i}\right)}{R'(-\beta_i)R''(\beta_i)(z-\beta_i)} \right].$$

The function $\Omega_3^{(0)}(u, v, z)$ is completely symmetric in its arguments.

In [10] also the solutions of $\Omega_m^{(g)}$ with $(g, m) = (0, 4), (1, 1)$ are derived, leading to the conjecture that meromorphic forms $\omega_{g,m}$ defined by $\omega_{0,1}(z) = -R(-z)R'(z)\mathrm{d}z$ and for $2g + m \geq 2$ by $\omega_{g,m}(z_1, \ldots, z_m) = \lambda^{2-2g-m}\Omega_m^{(g)}(z_1, \ldots, z_m)\prod_{j=1}^m R'(z_j)\mathrm{d}z_j$ follow blobbed topological recursion for the spectral curve

$$\left(x\colon \Sigma \to \Sigma_0, \omega_{0,1}(z), B(u, z)\right) = \left(R\colon \hat{\mathbb{C}} \to \hat{\mathbb{C}}, \; -R(-z)\mathrm{d}R(z), \; \frac{\mathrm{d}u\,\mathrm{d}z}{(u - z)^2}\right).$$

This means that the poles of $\omega_{g,m}$ at the ramification points β_i of R are given by the universal formula of topological recursion. These are enriched by further contributions which are holomorphic at β_i and have poles at $z_i = 0$ and $z_i + z_j = 0$ for the quartic Kontsevich model, starting with the appearance of some additional initial data in $\omega_{0,2}$, namely $\frac{\mathrm{d}u\,\mathrm{d}z}{(u+z)^2} = -B(u, -z)$ (Bergman kernel with one changed sign). Their general structure is not yet understood for $g > 0$, but we are confident that the following structures below extend to higher genera: The symmetry of the spectral curve, $y(z) = -x(-z)$ and $\omega_{0,2}(u, z) = B(u, z) - B(u, -z)$ gave the motivation to the deep involution identity [26]

$$\omega_{0,|I|+1}(I, q) + \omega_{0,|I|+1}(I, -q)$$
$$= -\sum_{s=2}^{|I|} \sum_{I_1 \uplus \cdots \uplus I_s = I} \frac{1}{s} \operatorname*{Res}_{z \to q} \left(\frac{\mathrm{d}R(-q)\mathrm{d}R(z)}{(R(-z) - R(-q))^s} \prod_{j=1}^s \frac{\omega_{0,|I_j|+1}(I_j, z)}{\mathrm{d}R(z)}\right) \tag{5.3}$$

completely determining the meromorphic forms $\omega_{0,m+1}$ by usual topological recursion (polar at β_i) and something surprisingly similar giving the holomorphic parts:

Theorem 5.3 ([26]). *Assume that $z \mapsto \omega_{0,n+1}(u_m, \ldots, u_m, z)$ is for $m \geq 2$ holomorphic at $z = -\beta_i$ and $z = u_k$ and has poles at most in points where the r.h.s. of* (5.3) *has poles. Then equation* (5.3) *is for $I = \{u_1, \ldots, u_m\}$ with $m \geq 2$ uniquely solved by*

$$\omega_{0,|I|+1}(I, z) = \sum_{i=1}^r \operatorname*{Res}_{q \to \beta_i} K_i(z, q) \sideset{}{'}\sum_{I_1 \uplus I_2 = I} \omega_{0,|I_1|+1}(I_1, q)\omega_{0,|I_2|+1}(I_2, \sigma_i(q))$$
$$- \sum_{k=1}^m \mathrm{d}_{u_k}\left[\operatorname*{Res}_{q \to -u_k} \sideset{}{'}\sum_{I_1 \uplus I_2 = I} \tilde{K}(z, q, u_k)\mathrm{d}_{u_k}^{-1}\left(\omega_{0,|I_1|+1}(I_1, q)\omega_{0,|I_2|+1}(I_2, q)\right)\right], \tag{5.4}$$

where the primed sum excludes the empty sets $I_i = \varnothing$.

Here $\sigma_i \neq \mathrm{id}$ denotes the local Galois involution in the vicinity of β_i, i.e., $R(\sigma_i(z)) = R(z)$, $\lim_{z \to \beta_i} \sigma_i(z) = \beta_i$. By d_{u_k} we denote the exterior differential in u_k. We had to introduce two recursion kernels of a similar structure:

$$K_i(z, q) := \frac{\frac{1}{2}\left(\frac{\mathrm{d}z}{z-q} - \frac{\mathrm{d}z}{z-\sigma_i(q)}\right)}{\mathrm{d}R(\sigma_i(q))(R(-\sigma_i(q)) - R(-q))}, \qquad \tilde{K}(z, q, u) := \frac{\frac{1}{2}\left(\frac{\mathrm{d}z}{z-q} - \frac{\mathrm{d}z}{z+u}\right)}{\mathrm{d}R(q)(R(u) - R(-q))}.$$

The linear and quadratic loop equations hold. We emphasise that Theorem 5.3 gives exactly the decomposition of $\omega_{0,m}$ into $\mathcal{P}_z\omega_{0,m} + \mathcal{H}_z\omega_{0,m}$ with projectors $\mathcal{P}_z$ and $\mathcal{H}_z$ on poles at the ramification points and the antidiagonal of a variable z. The kernels K and $\tilde{K}$ are constructed from the Bergman kernel $B(u, z)$ only, and not by the full $\omega_{0,2}$. This is a clear difference to the construction of Eynard and Orantin [18], which in this case would artificially produce (false) poles at negative ramification points. The blobs $\varphi_{g,n}$ in the sense of Borot and Shadrin [5] are defined as purely holomorphic part by the application of $\mathcal{H}_{z_i}$ on all m variables. This procedure is straightforward but will give a cumbersome result. Nevertheless we stress that

in the quartic Kontsevich model there is a remarkably simple rule to compute recursively the holomorphic part, which in the general theory are only mildly constrained by the quadratic loop equations.

The extension of (5.4) to $g \geq 1$ is work in progress. We refer to [17, 18] for topological recursion in general and to [5] for blobbed topological recursion.

5.2   Comparison between exact results and weighted ribbon graphs

In this subsection we compare the exact solutions of Theorem 5.1 and Proposition 5.2 with the perturbative expansion via weighted ribbon graphs. First, we need the expansion of ε_a and $R'(\varepsilon_a)$ which is easily obtained by iterative insertion into the definition of $R(z)$. The first orders yield:

$$
\varepsilon_q = e_q + \frac{\lambda}{N} \sum_{n=1}^{d} \frac{r_n}{e_q + e_n} - \frac{\lambda^2}{N^2} \sum_{n,k=1}^{d} r_n r_k \left(\frac{1}{(e_q + e_n)(e_k + e_n)^2} + \frac{1}{(e_q + e_n)^2(e_q + e_k)} \right.
$$
$$
\left. + \frac{1}{(e_q + e_n)^2(e_n + e_k)} \right) + \mathcal{O}(\lambda^3),
$$
$$
R'(\varepsilon_q) = 1 + \frac{\lambda}{N} \sum_{n=1}^{d} \frac{r_n}{(e_q + e_n)^2} - \frac{\lambda^2}{N^2} \sum_{n,k=1}^{d} r_n r_k \left(\frac{1}{(e_q + e_n)^2(e_k + e_n)^2} + \frac{2}{(e_q + e_n)^3(e_q + e_k)} \right.
$$
$$
\left. + \frac{2}{(e_q + e_n)^3(e_n + e_k)} \right) + \mathcal{O}(\lambda^3).
$$

Also necessary for $(g, n) = (0, 3)$ and higher topologies are the zeroes β_i of R' (so-called ramifications points). The λ-expansion yields

$$
\beta_i = -e_i + \mathrm{i}\sqrt{\frac{\lambda r_i}{N}} - \frac{\lambda}{N} \sum_{n=1}^{d} \frac{r_n}{e_i + e_n} + \mathcal{O}(\lambda^{\frac{3}{2}}), \qquad \beta_{i+d} = \bar{\beta}_i \qquad i \in \{1, \ldots, d\}. \tag{5.5}
$$

The expansions of ε_q and β_i are easily implemented into a computer algebra system. Deriving perturbative results for the $\Omega_n^{(g)}$ is then straightforward. We demonstrate this with the following examples:

Example 5.4. From the expansion of the exact result, we obtain using Theorem 5.1

$$
\Omega_1^{(0)}(\varepsilon_q) = \frac{\varepsilon_q - e_q}{\lambda} + \frac{1}{N} \sum_{n=1}^{d} r_n \left(\frac{1}{R'(\varepsilon_n)(\varepsilon_n - \varepsilon_q)} - \frac{1}{e_n - e_q} \right)
$$
$$
= \frac{1}{N} \sum_{n=1}^{d} \frac{r_n}{e_n + e_q} - \frac{\lambda}{N^2} \sum_{n,k=1}^{d} r_n r_k \left(\frac{1}{(e_q + e_n)(e_k + e_n)^2} + \frac{1}{(e_q + e_n)^2(e_q + e_k)} \right.
$$
$$
\left. + \frac{1}{(e_q + e_n)^2(e_n + e_k)} + \frac{1}{(e_n + e_k)^2(e_n - e_q)} + \frac{\frac{1}{e_n + e_k} - \frac{1}{e_q + e_k}}{(e_n - e_q)^2} \right) + \mathcal{O}(\lambda^2)
$$
$$
= \frac{1}{N} \sum_{n=1}^{d} \frac{r_n}{e_n + e_q} - \frac{\lambda}{N^2} \sum_{n,k=1}^{d} \left(\frac{r_n r_k}{(e_q + e_n)^2(e_q + e_k)} + \frac{r_n r_k}{(e_q + e_n)^2(e_n + e_k)} \right) + \mathcal{O}(\lambda^2).
$$

This result is in full compliance with the graph expansion of Example 3.5 inserted into $\Omega_q^{(0)} = \frac{1}{N} \sum_{k=1}^{N} G_{|qk|}^{(0)}$. The agreement is immediate for $r_n = 1$; otherwise one collects r_k identical terms, where $E_{k_1} = \cdots = E_{k_{r_k}} = e_k$. The expansion of the exact result is represented in a different partial fraction decomposition than the graph expansion. The reader may check also the next order.

Example 5.5. We obtain from Proposition 5.2

$$\Omega_2^{(0)}(\varepsilon_q, \varepsilon_r) - \frac{1}{(e_q - e_r)^2} = \frac{1}{R'(\varepsilon_q)R'(\varepsilon_r)}\left(\frac{1}{(\varepsilon_q - \varepsilon_r)^2} + \frac{1}{(\varepsilon_q + \varepsilon_r)^2}\right) - \frac{1}{(e_q - e_r)^2}$$

$$= \frac{1}{(e_q + e_r)^2} - \frac{\lambda}{N}\sum_{n=1}^{d} r_n\left(2\frac{\frac{1}{e_n+e_q} - \frac{1}{e_n+e_r}}{(e_q - e_r)^3} + \frac{\frac{1}{(e_q+e_n)^2} + \frac{1}{(e_r+e_n)^2}}{(e_q - e_r)^2}\right.$$

$$\left. + 2\frac{\frac{1}{e_n+e_q} + \frac{1}{e_n+e_r}}{(e_q + e_r)^3} + \frac{\frac{1}{(e_q+e_n)^2} + \frac{1}{(e_r+e_n)^2}}{(e_q + e_r)^2}\right) + \mathcal{O}(\lambda^2),$$

which is in full compliance with the graph expansion of Examples 3.5 and 3.6 inserted into Proposition 4.7 (but in a different partial fraction decomposition). The reader may check the next order, where additionally the graphs of the $(2+2)$-point function from Example 3.7 contribute.

Example 5.6. We obtain from Proposition 5.2

$$\Omega_3^{(0)}(\varepsilon_q, \varepsilon_r, \varepsilon_s) = \frac{1}{R'(\varepsilon_q)R'(\varepsilon_r)R'(\varepsilon_s)}\left[\frac{\partial}{\partial u}\frac{\lambda\left(\frac{1}{(\varepsilon_r+u)^2} + \frac{1}{(\varepsilon_r-u)^2}\right)}{R'(u)R'(-u)(\varepsilon_s + u)^2}\bigg|_{u=\varepsilon_q}\right.$$

$$+ \frac{\partial}{\partial v}\frac{\lambda\left(\frac{1}{(\varepsilon_q+v)^2} + \frac{1}{(\varepsilon_q-v)^2}\right)}{R'(v)R'(-v)(\varepsilon_s + v)^2}\bigg|_{v=\varepsilon_r}$$

$$\left. - \sum_{i=1}^{2d}\frac{\lambda\left(\frac{1}{(\varepsilon_r+\beta_i)^2} + \frac{1}{(\varepsilon_r-\beta_i)^2}\right)\left(\frac{1}{(\varepsilon_q+\beta_i)^2} + \frac{1}{(\varepsilon_q-\beta_i)^2}\right)}{R'(-\beta_i)R''(\beta_i)(\varepsilon_s - \beta_i)^2}\right]$$

$$= -\lambda \cdot 2\left(\frac{\frac{1}{(e_r+e_q)^2} + \frac{1}{(e_r-e_q)^2}}{(e_s + e_q)^3} + \frac{\frac{1}{(e_r+e_q)^3} - \frac{1}{(e_r-e_q)^3}}{(e_s + e_q)^2}\right.$$

$$\left. + \frac{\frac{1}{(e_q+e_r)^2} + \frac{1}{(e_q-e_r)^2}}{(e_s + e_r)^3} + \frac{\frac{1}{(e_q+e_r)^3} - \frac{1}{(e_q-e_r)^3}}{(e_s + e_r)^2}\right) + \mathcal{O}(\lambda^2),$$

where the restrictions to $u = \varepsilon_q$ and $v = \varepsilon_r$ in the second line vanish. The only contributions come from the i-summation. This result is in full compliance with the graph expansion in Examples 3.5 and 3.6 inserted into Proposition 4.8, but again in a different partial fraction decomposition. For the computation, we remark that the expansion

$$\frac{1}{(\varepsilon_q + \beta_q)^2} = -\frac{N}{\lambda r_q} + \mathcal{O}\left(\frac{1}{\sqrt{\lambda}}\right), \qquad \frac{1}{(\varepsilon_q + \beta_{q+d})^2} = -\frac{N}{\lambda r_q} + \mathcal{O}\left(\frac{1}{\sqrt{\lambda}}\right),$$

$$\frac{1}{R''(\beta_i)} = -\frac{i}{2}\sqrt{\frac{\lambda r_i}{N}} + \mathcal{O}(\lambda), \qquad \frac{1}{R''(\beta_{i+d})} = \frac{i}{2}\sqrt{\frac{\lambda r_i}{N}} + \mathcal{O}(\lambda)$$

indicates a contribution of order $\sqrt{\lambda}$ from the i-summation, which actually cancels due to the pairs (β_i, β_{i+d}) of complex conjugations $\bar{\beta}_i = \beta_{i+d}$. The reader may even check that the order $\lambda^{\frac{3}{2}}$ cancels as well.

5.3 Combinatorics

A common investigation in QFT concerns the growth of the number of Feynman graphs at a certain order λ^v. In order to illustrate the enormous complexity of the individual contributions to $\Omega_q^{(0)}$ and $\Omega_{q_1,q_2}^{(0)}$ at a given order λ^v, we will calculate these numbers explicitly. To enter this regime of enumerative geometry within the quartic Kontsevich model we have to set $d = 1$. We will now show how to expand $G_{|11|}^{(0)}$, $G_{|1111|}^{(0)}$ and $G_{|11|11|}^{(0)}$ (the 2-point, 4-point and $(2+2)$-point

function for a single, $(r_1=N)$-fold degenerate spectral value $e_1 = e$) in an exact and generic per-turbative series in λ. The prefactors of $(-\lambda)^v$ for $e = \frac{1}{2}$ then simply *count* the number of connected Feynman ribbon graphs contributing to the graph expansion at order v. As known from the Hermitian 1-matrix model [11], the duals of the ribbon graphs of the quartic Kontse-vich model are rooted quadrangulations. However, due to a different definition of correlation functions, the correspondence to [11] is not one-to-one.[6] To avoid complicated redefinitions, we follow another path.

To derive the exact power series in λ, return to Theorem 5.1 and solve the $2d$ implicitly defined equations for $d = 1$ explicitly. For $\varepsilon_1 = \varepsilon$, we solve them to

$$\varepsilon = \frac{1}{6}\big(4e + \sqrt{4e^2 + 12\lambda}\big), \qquad \varrho = \frac{N}{18\lambda}\big(2e\sqrt{4e^2 + 12\lambda} - 4e^2 + 12\lambda\big).$$

With the other preimage $\hat{\varepsilon} = -\frac{1}{6}\big(2e + 2\sqrt{4e^2 + 12\lambda}\big)$ one expresses[7] the planar 2-point function as

$$G_{|11|}^{(0)} \equiv G^{(0)}(e,e) \equiv G^{(0)}(R(\varepsilon), R(\varepsilon)) =: \mathcal{G}^{(0)}(\varepsilon, \varepsilon) = -\frac{2\hat{\varepsilon}}{(\varepsilon - \hat{\varepsilon})^2}.$$

Admitting multiplicities r_k in the definition (4.1) of $\Omega_q^{(0)}$ we find for $d = 1$ and $r_1 = N$

$$\Omega_q^{(0)} = \frac{1}{N}\sum_{k=1}^{d} r_k G_{|qk|}^{(0)} \longrightarrow \Omega_1^{(0)} = G_{|11|}^{(0)} = \mathcal{G}^{(0)}(\varepsilon, \varepsilon).$$

The same steps give for $\Omega_{q_1,q_2}^{(0)}$ according to Proposition 4.7

$$\Omega_{q_1,q_2}^{(0)} = \frac{1}{(e_{q_1} - e_{q_2})^2} + \big(G_{|q_1 q_2|}^{(0)}\big)^2 + \frac{1}{N}\sum_{k=1}^{N} r_k \Big(G_{|q_1 k q_1 q_2|}^{(0)} + G_{|q_2 k q_2 q_1|}^{(0)} + G_{|q_1 k q_2 k|}^{(0)}\Big)$$

$$+ \frac{1}{N^2}\sum_{k,l=1}^{N} r_k r_l G_{|q_1 k|q_2 l|}^{(0)} \longrightarrow \lim_{e_{q_1},e_{q_2}\to e}\Big(\Omega_{q_1,q_2}^{(0)} - \frac{1}{(e_{q_1} - e_{q_1})^2}\Big)$$

$$= \mathcal{G}^{(0)}(\varepsilon, \varepsilon)^2 + 3\mathcal{G}^{(0)}(\varepsilon, \varepsilon, \varepsilon, \varepsilon) + \mathcal{G}^{(0)}(\varepsilon, \varepsilon|\varepsilon, \varepsilon).$$

A lengthy calculation shows

$$\mathcal{G}^{(0)}(\varepsilon, \varepsilon, \varepsilon, \varepsilon) = \frac{8e + 12\sqrt{4e^2 + 12\lambda}}{\big(2e + \sqrt{4e^2 + 12\lambda}\big)^3} - 2\big(\mathcal{G}^{(0)}(\varepsilon, \varepsilon)\big)^2,$$

$$\mathcal{G}^{(0)}(\varepsilon, \varepsilon|\varepsilon, \varepsilon) = \frac{6\lambda^2}{\big(e + \sqrt{4e^2 + 12\lambda}/2\big)^6}. \tag{5.6}$$

Inserting the λ-expansion of these formulae above gives the number of ribbon graphs contributing to $\Omega_q^{(0)}$ and $\Omega_{q_1,q_2}^{(0)}$ at a given order λ^v. In the following table we list these numbers up to order λ^5, including also $\Omega_{q_1,q_2,q_3}^{(0)}$ for completeness.

---

[6]For the Hermitian 1-matrix model one usually considers resolvents which from a combinatorial perspective are sometimes called ordinary maps. Our correlation correspond for $d = 1$ to the so-called fully simply maps, see [4] for precise definitions.

[7]See [10] for details about the complexification procedure from correlation functions $G_{...}^{(g)}$ to meromorphic functions $\mathcal{G}^{(g)}(\dots)$.

Order	$\Omega_q^{(0)}$	$\Omega_{q_1,q_2}^{(0)} = \left(\Omega_{q_1,q_2}^{(0)}\right)^{\mathrm{TR}} + \left(\Omega_{q_1,q_2}^{(0)}\right)^{\mathrm{BTR}}$	$\Omega_{q_1,q_2,q_3}^{(0)}$
λ^0	1	$1 = 0 + 1$	0
λ^1	2	$7 = 1 + 6$	4
λ^2	9	$58 = 13 + 45$	84
λ^3	54	$522 = 144 + 378$	1322
λ^4	378	$4941 = 1539 + 3402$	18684
λ^5	2916	$48411 = 16335 + 32076$	249156

Those numbers can be checked at low orders of λ counting the diagrams in Figures 3, 4 and 5. Regarding $\Omega_q^{(0)}$ we encounter very special numbers. By duality these are the same as the numbers $m_{g=0}(n)$ of planar ($g = 0$) quadrangulations with n faces plus a (marked) boundary of length 2. We recall:

Theorem 5.7 ([17, Chapter 3.1.7]). *The number of rooted quadrangulations of the sphere with n quandrangles is given by*

$$2 \cdot 3^n \cdot \frac{(2n)!}{n!(n+2)!} = 2 \cdot 3^n \cdot \frac{C_n}{n+2}$$

with the Catalan number C_n.

The planar 2-point function for $d = 1$ itself generates these numbers together with weights $\frac{1}{2e}$ of the edges.

The result for the number of ribbon graphs of order λ^n contributing to $\Omega_{1,1}^{(0)}$ (we splitted the number into the usual Bergman kernel and the blob) can be derived from the Taylor series of (5.6) whose first terms are

$$\mathcal{G}^{(0)}(\varepsilon, \varepsilon | \varepsilon, \varepsilon) = \frac{6(-\lambda)^2}{(2e)^6} + \frac{108(-\lambda)^3}{(2e)^8} + \frac{1458(-\lambda)^4}{(2e)^{10}} + \frac{17820(-\lambda)^5}{(2e)^{12}} + \cdots,$$

$$\mathcal{G}^{(0)}(\varepsilon, \varepsilon, \varepsilon, \varepsilon) = \frac{(-\lambda)}{(2e)^4} + \frac{10(-\lambda)^2}{(2e)^6} + \frac{90(-\lambda)^3}{(2e)^8} + \frac{810(-\lambda)^4}{(2e)^{10}} + \frac{7425(-\lambda)^5}{(2e)^{12}} + \cdots.$$

These numbers give experimental evidence for the footnote from above that $G_{|p_1^1 \cdots p_{n_1}^1 | \cdots | p_1^b \cdots p_{n_b}^b|}^{(g)}$ are generating series of *fully simple maps*. Building on results concerning quadrangulations from Bernardi and Fusy [3], we can express the above series in a closed form:

$$\mathcal{G}^{(0)}(\varepsilon, \varepsilon | \varepsilon, \varepsilon) = 4 \binom{3}{1}^2 \sum_{m=0}^{\infty} \frac{3^m (6 + 2m - 1)!}{m!(6 + m)!} \frac{(-\lambda)^{m+2}}{(2e)^{2m+6}},$$

$$\mathcal{G}^{(0)}(\varepsilon, \varepsilon, \varepsilon, \varepsilon) = \frac{6!}{3!2!} \sum_{m=0}^{\infty} \frac{3^{m-1}(3 + 2m)!}{m!(5 + m)!} \frac{(-\lambda)^{m+1}}{(2e)^{2m+4}}.$$

The separation into pure TR and BTR additions and its combinatorial interpretation is work in progress.

A more sophisticated generating function takes also the non-trivial automorphism groups of connected closed ribbon graphs into account – the *free energy* $\mathcal{F}^{(g)}$. As a final illustration, we will reproduce the power series of planar closed ribbon graphs of Figure 2 using a representation of $\mathcal{F}^{(0)}$. For this object, we need to define a couple of quantities that are based on the general results of [18]:

Definition 5.8. Consider the poles $a = \{\pm\varepsilon_i, \infty\}$ of $\omega_{0,1}(z) = -R(-z)R'(z)$. Define the

- *temperatures* by $t_a = \operatorname{Res}_{z \to a} \omega_{0,1}(z)$;
- *local variables* for poles of $R'(z)$ via $\xi_a(z) = \frac{1}{R(z)}$ and for poles of $R(-z)$ via $\xi_a(z) = \frac{1}{R(z) - R(a)}$;
- *potential*

$$
V_a(z) = \operatorname{Res}_{q \to a} \omega_{0,1}(q) \log\left(1 - \frac{\xi_a(z)}{\xi_a(q)}\right) = \sum_{k=1}^{\deg V_a} t_{a,k} \xi_a^k(z),
$$

  where $t_{a,k}$ defines the *moduli* of the pole a;
- *loop annihilation operator* by the primitive of $\omega_{0,1}(z)$:

$$
\Phi(z) = \int^{z'=z} \omega_{0,1}(z') = \frac{z^2}{2} + \frac{\lambda}{N} \sum_k \left[\frac{r_k R(\varepsilon_k)}{R'(\varepsilon_k)(z + \varepsilon_k)} + r_k \log\left(\frac{z + \varepsilon_k}{z - \varepsilon_k}\right) \right].
$$

Using these objects, we can formulate the genus zero free energy:

$$
\mathcal{F}^{(0)} = \frac{1}{2} \sum_a \left[\operatorname{Res}_{q \to a} \omega_{0,1}(q) V_a(q) + t_a \mu_a \right] + \mathcal{R}, \qquad \mu_a := \lim_{q \to a} \left(V_a(q) - t_a \log[\xi_a(q)] - \Phi(q) \right).
$$

It is necessary to add a compensating term $\mathcal{R} := -\frac{\lambda}{2N} \sum_k r_k e_k^2 + \frac{\lambda^2}{2N^2} \sum_{k,i} r_i r_k \log(e_i - e_k)$ since $\Omega_1^{(0)}(z)$ differs from $-R(-z)$ (recall $\omega_{0,1}(z) = -R(-z)R'(z)$). Acting with the creation operator on $\mathcal{R}$ exactly yields the additional terms in (5.1):

$$
\frac{\partial \mathcal{R}}{\partial e_b} = \Omega_1^{(0)}(\varepsilon_b) + R(-\varepsilon_b)
$$

giving rise to a well-defined initial data also at $z = \varepsilon_b$, where $R(-z)$ itself becomes singular.

For our purposes, set again $d = 1$ and calculate $t_{\pm\varepsilon} = \mp\lambda$, $t_\infty = 0$ as well as $V_\varepsilon(z) = 0$, $V_{-\varepsilon}(z) = -e_1 \cdot R(z)$, $V_\infty(z) = \frac{R(z)^2}{2}$. Only the residue for the pole $-\varepsilon$ gives a contribution, namely $\frac{\lambda\rho}{16\varepsilon^4}\left(16\varepsilon^6 - 4\varepsilon^4\lambda\rho + (\lambda\rho)^3\right)$. We also calculate

$$
t_\varepsilon \mu_\varepsilon + t_{-\varepsilon} \mu_{-\varepsilon} = \lambda\left[\varepsilon^2 - \frac{\lambda^2\rho^2}{4\varepsilon^2} + \lambda \log\left(1 + \frac{4\varepsilon^2}{\lambda\rho}\right)\right].
$$

Inserting the explicit solutions for ϵ and ρ and taking the compensation $\mathcal{R}$ into consideration, we can expand the result in a power series:

$$
\mathcal{F}^{(0)} = \sum_{n=1}^{\infty} 3^n \frac{(2n-1)!}{n!(n-2)!} \frac{(-\lambda)^n}{(2e)^{2n}}
$$
$$
= \frac{-\lambda}{2(2e)^2} + \frac{9(-\lambda)^2}{8(2e)^4} + \frac{9(-\lambda)^3}{2(2e)^6} + \frac{189(-\lambda)^4}{8(2e)^8} + \frac{729(-\lambda)^5}{5(2e)^{10}} + \cdots.
$$

We encounter, e.g., the automorphism groups $\frac{1}{2} + \frac{1}{2} + \frac{1}{8}$ of the graphs at $\mathcal{O}(\lambda^2)$ in Figure 2. Again, we can cite a former result from the Hermitian 1-matrix model:

Proposition 5.9 ([17, Chapter 3.6.1]). *The generating function of non-rooted quadrangulations of the sphere reads, including automorphism groups:*

$$
\frac{1}{6\left(1 + \sqrt{1 - 12\lambda}\right)^2} - \frac{5}{6\left(1 + \sqrt{1 - 12\lambda}\right)} + \frac{3}{8} - \frac{\log\left(1 + \sqrt{1 - 12\lambda}\right)}{4}.
$$

Our expression of $\mathcal{F}^{(0)}$ is at first sight far more complicated, but can be reduced to this expression – the power series of both expressions are equal (up to a sign of λ). Deriving the result with respect to e proves again the correct action of the creation operator becoming a trivial derivative for closed graphs: one recovers the numbers $2, 9, 54, 378, \ldots$ from Lemma 5.7.

Remark 5.10. Despite the appearance of blobbed topological recursion in our model, $\mathcal{F}^{(0)}$ fits into the usual picture of topological recursion for obvious reasons. However, the other special free energy $\mathcal{F}^{(1)}$ needs additional terms responsible for the blob (work in progress).

6 Critical coupling constants and geometric discussion

So far, we were able to show analytically the expected coincidence between the exact solutions from (blobbed) topological recursion of the quartic Kontsevich model and their perturbative expansion in the coupling constant λ. Many systems of statistical physics, quantum mechanics and quantum field theory show critical phenomena and phase transitions when parameters take particular values. This section starts to explore such phenomena in the quartic Kontsevich model. More precisely, we exemplify transitions between different stratification types of the parameter space. This includes the appearance of higher-order ramifications in the crucial function R identified in Theorem 5.1 and transitions between different ramification profiles.

6.1 The setup

The investigation of special cases of the quartic Kontsevich model already suggested certain values of λ at which a critical behaviour occurs. In [21] a scaling limit $d, N \to \infty$ of (5.2) to a renormalised integral representation $R(z) = z - \lambda(-z)^{D/2} \int_0^\infty \frac{\varrho(t)\mathrm{d}t}{(t+1)^{D/2}(t+1+z)}$ was established, with $D \in \{0, 2, 4\}$ the smallest dimension that gives a convergent integral. We recall:

- Let $d = 1$ with an N-fold degenerate eigenvalue [21]. This is the Hermitian 1-matrix model. We obtain $R(\varepsilon) = \varepsilon - \frac{\lambda}{N} \frac{\varrho}{2\varepsilon} = e$, where $\frac{N}{\varrho} = R'(\varepsilon)$, with solution $\varepsilon = \left(e + \sqrt{4e^2 + 12\lambda} \right)/6$ directly given by inversion of R. In standard conventions one should identify $e = \frac{1}{2}$ which gives a critical value $\lambda_c = -\frac{1}{12}$ below which R^{-1} cannot be defined as map between real functions.

- Let $d \to \infty$ with spectral measure $\varrho(t) = 1$, the two-dimensional Moyal plane. After renormalisation one obtains $R(z) = z + \lambda \log(1 + z)$ [31]. An integral representation for the planar 2-point function is only consistent for $\lambda > -\frac{1}{\log(4)}$.

- Let $d \to \infty$ with spectral measure $\varrho(t) = t$, the four-dimensional Moyal plane: One finds $R(z) = z\,_2F_1(\alpha_\lambda, 1 - \alpha_\lambda, 2; -z)$, where $\alpha_\lambda = \arcsin(\lambda\pi)/\pi$ for $|\lambda| \leq \frac{1}{\pi}$ and $\alpha_\lambda = \frac{1}{2} + \mathrm{i}\,\mathrm{arcosh}(\lambda\pi)/\pi$ for $\lambda \geq \frac{1}{\pi}$ [22]. The singular value is $\lambda_s = -1/\pi$. Its mirror $\lambda_{\mathrm{crit}} = +\frac{1}{\pi}$ is a special transition point, where α_λ is continuous but not differentiable. However, $R(z)$ itself crosses smoothly over λ_{crit}.

Beyond these special cases, we mostly leave the realm of exact solutions. Existence of solutions in a real or complex neighbourhood of $\lambda = 0$ is guaranteed by the implicit function theorem which constructs $2d$ functions $\{\varepsilon_k(\lambda), \varrho_k(\lambda)\}_{k=1,\ldots,d}$ from given data $e_k, r_k = \lim_{\lambda \to 0}(\varepsilon_k, \varrho_k)$. For a first discussion we simplify the situation and take $(\varepsilon_k, \varrho_k)$ as given data independently of λ. This ignores the condition $r_k \in \mathbb{Z}_{>0}$ (could be arbitrarily well approximated for $N \to \infty$). We will mostly consider the case $d = 2$.

6.2   Behaviour of the Ramification points for $d = 2$

The case $d = 2$ describes a threefold covering and four ramification points. We scan the running of the ramification points $\beta_{1,2}$ and their complex conjugate by a variation of the coupling constant. Because of $-2\sum_{k=1}^{d} \varepsilon_k = \sum_{i=1}^{2d} \beta_i$ (underpinning the perturbative expansions), which is a consequence of Vieta's theorem, the variations of the β_i sum up to zero. Figure 7 shows the typical situation. We rediscover the square root-like behaviour (5.5) for small λ.
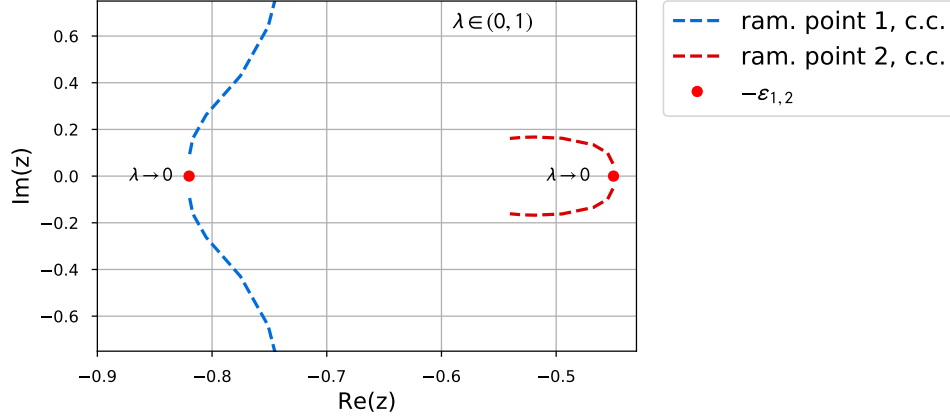
Figure 7.   For $\lambda \to 0$, the ramification points propagate into $-\varepsilon_1 = -0.82$ and $-\varepsilon_2 = -0.45$ (these values for ε_i are also chosen in Figures 11 and 12, as well as $\varrho_1 = 1$, $\varrho_2 = 3$). In sum, the deformations average to zero.

Taking $\varrho_1 = \varrho_2$, we reenter the regime of analytically solvable equations. Over and above, it shows a phenomenologically new behaviour:

Lemma 6.1. *Given $d = 2$ parameters $\varepsilon_1 \neq \varepsilon_2$ and suppose their multiplicities arrange to $\varrho_1 = \varrho_2 =: N\varrho$. Then two ramification points merge to a single higher ramification point $\beta = \beta_1 = \beta_2$ at the critical coupling constant $\lambda_{\mathrm{crit}} = \frac{(\varepsilon_1 - \varepsilon_2)^2}{\varrho}$. Its real part is a fixed point $R(\mathrm{Re}(\beta)) = \mathrm{Re}(\beta)$ of R.*

Proof.   The value λ_{crit} is determined as follows: The four solutions of $R'(z) = 0$ read

$$\beta_{\pm,\pm} = \frac{1}{2}\left(-\varepsilon_1 - \varepsilon_2 \pm \sqrt{(\varepsilon_1 + \varepsilon_2)^2 - 4\left[\varepsilon_1\varepsilon_2 + \lambda\varrho \pm \sqrt{-\lambda\varrho(\varepsilon_1 - \varepsilon_2)^2 + \lambda^2\varrho^2}\right]}\right).$$

Then $\lambda = 0$ and $\lambda_{\mathrm{crit}} = \frac{(\varepsilon_1 - \varepsilon_2)^2}{\varrho}$ are the solution where two roots merge. Let β_1, β_2 be the solutions in the upper half plane. Then $\mathrm{Im}(\beta_1) = \mathrm{Im}(\beta_2) > 0$ for $\lambda < \lambda_{\mathrm{crit}}$ and $\mathrm{Re}(\beta_1) = \mathrm{Re}(\beta_2) = -\frac{\varepsilon_1 + \varepsilon_2}{2} =: -\bar{\varepsilon}$ for $\lambda > \lambda_{\mathrm{crit}}$. For obvious reasons this value is a fixed point of R, i.e., $R(-\bar{\varepsilon}) = -\bar{\varepsilon}$. This order-two ramification can be plotted as in Figure 8.   ∎

We exemplify the possibility of smooth interpolations of λ around the critical coupling λ_{crit} by applying the theory of higher-order ramifications in topological recursion (intensely studied [6]) giving $\omega_{0,3}[\lambda_{\mathrm{crit}}]$ compared with the limit $\lim_{\lambda \to \lambda_{\mathrm{crit}}} \omega_{0,3}[\lambda]$ of the standard result of simple ramifications:

Example 6.2 (for general d).   Consider two zeroes each of degree d of $R'(z)$, named $\beta_\pm$. The poles of $\omega_{0,3}(u, v, z)$ at $z + u = 0$ and $z + v = 0$ are not affected by higher-order ramifications. We thus only concentrate on the part $\mathcal{P}_z\omega_{0,3}(u, v, z)$ of $\omega_{0,3}(u, v, z)$ which collects
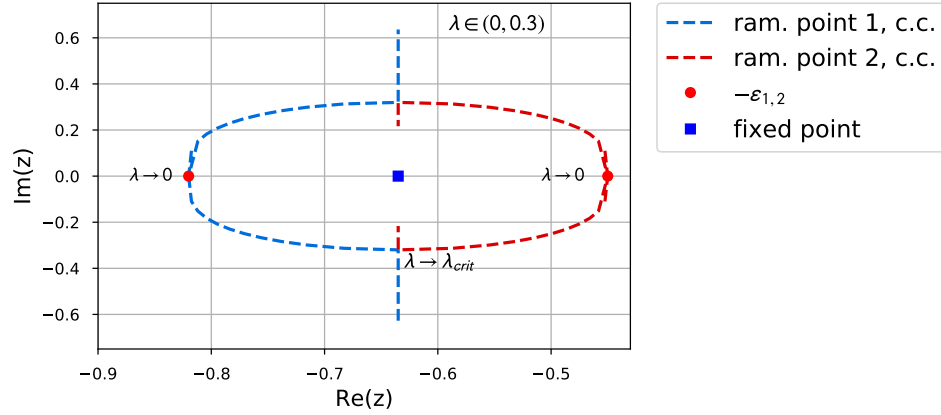
Figure 8. Running of ramification points for $d = 2$ and identical $\varrho := \frac{\varrho_1}{N} = \frac{\varrho_2}{N} = 2$. The critical coupling constant is $\lambda_{\text{crit}} = \frac{(\varepsilon_1 - \varepsilon_2)^2}{\varrho}$. For $\lambda > \lambda_{\text{crit}}$ the ramification points have constant real part $-\frac{\varepsilon_1 + \varepsilon_2}{2}$. At λ_{crit} itself, topological recursion has to be modified to the variant of *higher-order ramifications*.

the residues at $z = \beta_\pm$. Apply [7, Definition 3.6] for the topological recursion of higher-order ramification to obtain

$$\mathcal{P}_z \omega_{0,3}(u, v, z) = \operatorname*{Res}_{q \to \beta_\pm} \sum_{j=1}^{d} \mathrm{d}q \, K_2(z, q, \hat{q}^j) \omega_{0,2}(q, u) \omega_{0,2}(\hat{q}^j, v) + \{u \leftrightarrow v\},$$

$$K_2(z, q, \hat{q}^j) = \frac{\mathrm{d}z}{2R'(\hat{q}^j)(R(-q) - R(-\hat{q}^j))} \cdot \left(\frac{1}{z - q} - \frac{1}{z - \hat{q}^j} \right)$$

with the ordinary *Eynard kernel* $K_2 = K$ in the language of [7] (generalised kernels are not necessary for $n = 3$) and the preimages $\hat{z}^j$ of $R(z) = R(\hat{z}^j)$ with $\hat{z}^j \to \beta_\pm$ $\forall j$ for $z \to \beta_\pm$, $z \neq \hat{z}^j$. This gives rise to d-fold ramification at each fixed point. Next, we simplify the recursion kernel by expansion around the pole at $\beta_\pm$. The residue for $\mathcal{P}_z \omega_{0,3}(u, v, z)$ gives the same term for every d summands (same fixed point of all involutions):

$$\mathcal{P}_z \omega_{0,3}(u, v, z) = d \times \frac{\omega_{0,2}(u, \beta_+) \omega_{0,2}(v, \beta_+)}{R''(\beta_+) R'(-\beta_+)(z - \beta_+)} + [\beta_+ \leftrightarrow \beta_-].$$

This is of course the same as if one would set $\beta_i = \beta_+$, $\beta_{i+d} = \beta_-$ $\forall i$ into 5.2 afterwards being the limit $\lim\limits_{\lambda \to \lambda_{\text{crit}}} \mathcal{P}_z \omega_{0,3}(u, v, z)$.

This is no accident: the formula was designed to give continuity in the parameter which causes higher-order ramification, i.e., $\lim\limits_{\lambda \to \lambda_{\text{crit}}} \omega_{g,n}[\lambda] = \omega_{g,n}[\lambda_{\text{crit}}]$, and as said before, additional blob contributions are not affected by higher-order ramifications. Since our spectral curve is *acceptable* in the sense of [6, Definition 8], everything works also for our model with blobs.

6.3 Conformal mapping of the branch cuts

Nikolai Zhukovsky found a suitable conformal map to solve the potential flow of certain airfoils in an easier way [34]. It transforms an infinitely thin wing into a circular one. During the analysis of the Hermitian 1-matrix model, one recognised that this Zhukovsky transform occurs in the spectral curve $x(z)$ and conformally maps the domain around the branch cut into the exterior of the unit disk [17, Section 3.1]. We will take this prime example to perform a more detailed analysis for our $x(z) = R(z)$ with d branch cuts and $d + 1$ sheets. Let $d = 2$ from
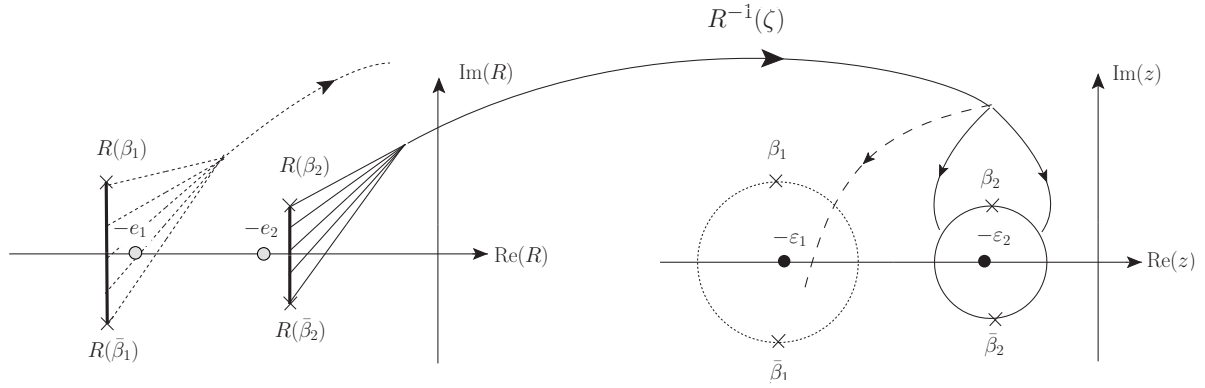
Figure 9. In the R-plane, we determine the branch cut to be the vertical connection between $R(\beta_i)$ and $R(\bar{\beta}_i)$, with $\mathrm{Im}(\bar{\beta}_i) = -\mathrm{Im}(\beta_i)$. The inverse R^{-1} pulls back the branch cut into the z-plane and causes $d+1$ preimages for d distinct values e_k. For small λ, small circles are generated. The remaining $d-1$ preimages of the cut are arcs located inside each of the other $d-1$ disks. They are not shown in the picture. We illustrated $d = 2$.
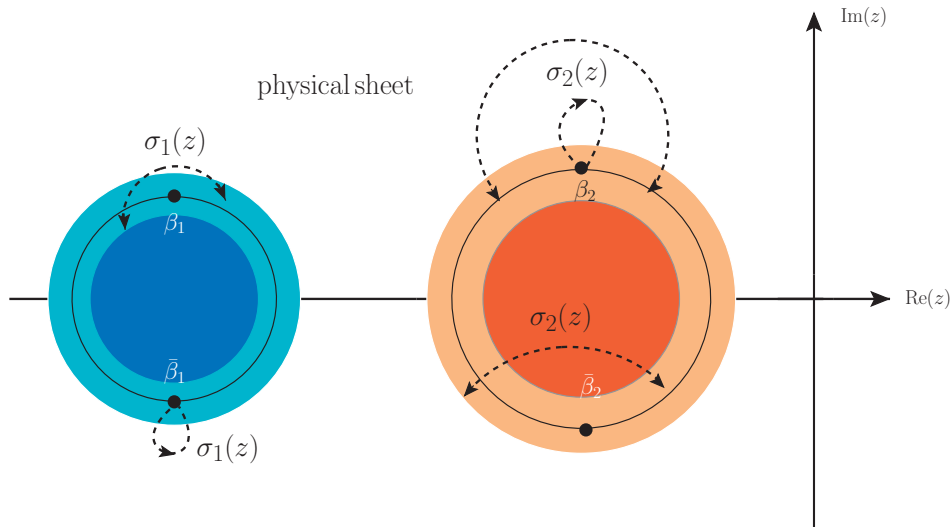
Figure 10. The preimage of $\hat{\mathbb{C}} \setminus \{\Gamma_1 \cup \Gamma_2\}$ under a ramified covering of degree 3 distinguishes two (deformed) closed disks $\mathbb{D}_i$ in the z-plane. In a neighbourhood of their boundaries, the Galois involutions $\sigma_{1,2}(z)$ allow to communicate with the physical sheet $\hat{\mathbb{C}} \setminus \{\mathbb{D}_1 \cup \mathbb{D}_2\}$. Their fixed points β_i, $\bar{\beta}_i$ mark north and south pole of $\mathbb{D}_i$.

now on. We choose to fix $\varepsilon_{1,2}$ and $\varrho_{1,2}$ and pull the branch cuts back into the z-plane – ending up with three preimages/sheets. This procedure is sketched in Figure 9.

More formally: We map the domain $\hat{\mathbb{C}} \setminus \{\Gamma_1 \cup \Gamma_2\}$ with $\Gamma_i := \left[R(\beta_i), R(\bar{\beta}_i) \right]$ as segments of $i\mathbb{R}$ into the exterior of the λ-deformed closed disks $\mathbb{D}_i$ – the *physical sheet*. In this sheet, we have a biholomorphic map $R^{-1} \colon \hat{\mathbb{C}} \setminus \{\Gamma_1 \cup \Gamma_2\} \to \hat{\mathbb{C}} \setminus \{\mathbb{D}_1 \cup \mathbb{D}_2\}$ sending ∞ to ∞.

Figure 10 illustrates the Galois involutions $\sigma_i(z)$, which are holomorphic local involutions with fixed points β_i and $\bar{\beta}_i$. They fulfil $R(\sigma_i(z)) = R(z)$ with $\sigma_i(z) \neq \mathrm{id}$. These involutions (special deck transformations) are crucial to formulate topological recursion and let the interior and exterior of the deformed discs communicate.

After this prelude, we continue with the numerical analysis and take around 20 images in the R-plane along the branch cuts from $R(\beta_i)$ to $R(\bar{\beta}_i)$ and map them with R^{-1} into the z-plane.

A first analysis with increasing coupling constant λ yields circle-like objects growing in radius and deformation (Figure 11).
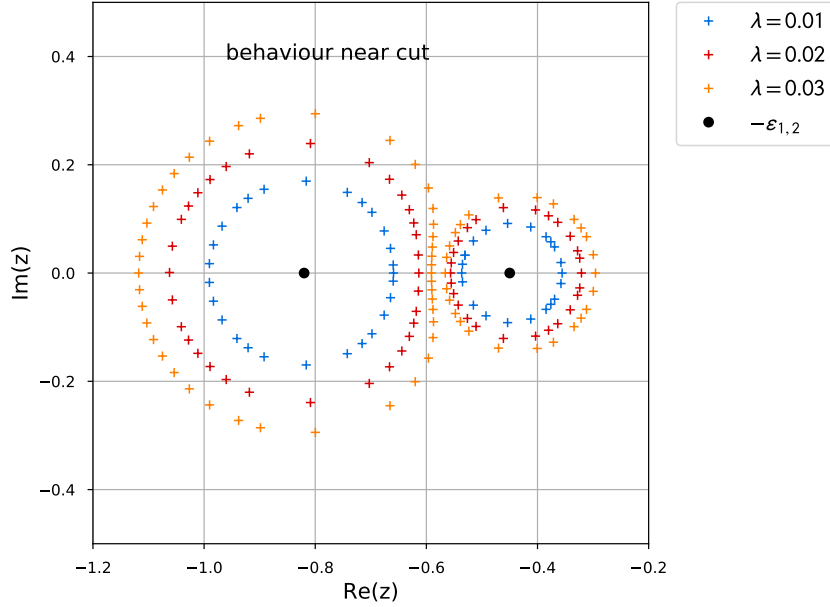

Figure 11. We choose $-\varepsilon_1 = -0.82$ and $-\varepsilon_2 = -0.45$ and draw the preimages of a cut between $R(\beta_i)$ and $R(\overline{\beta_i})$. The corresponding arcs from z and $\sigma_i(z)$ form deformed circles. Their deformation increases with λ and evolves by avoiding any intersection/collision of the two circles. A larger gap between ε_1 and ε_2 allows for stronger couplings before reaching a critical regime. The third preimage $\hat{z}$ (different from z, $\sigma_i(z)$ forms an arc inside the other circle and is not given in this figure.

We observe that the radius of the deformed circles is mainly determined by the multiplicity ϱ_k. The two branch cuts come closer to each other as λ increases; they merge at a critical value λ_{crit}. For $\lambda > \lambda_{\text{crit}}$ a stunning change of shape to an *avocado plot* occurs, see Figure 12.
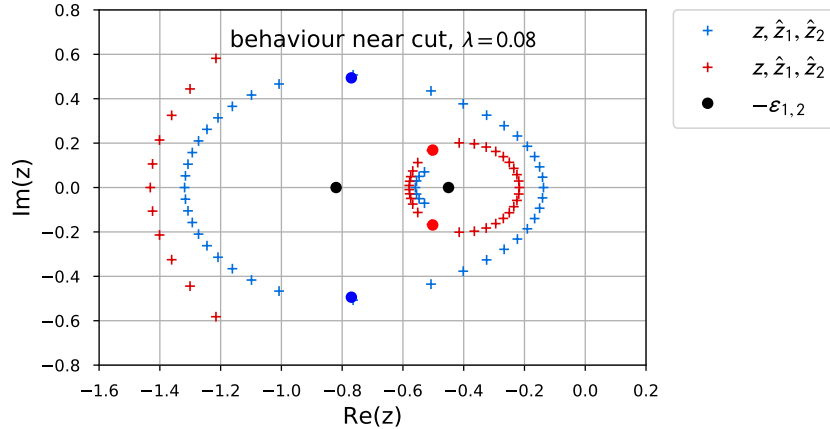
Figure 12. For $\lambda > \lambda_{\text{crit}}$ a change of shape to an *avocado* plot occurs. For the core, the local Galois involution communicates between core and flesh. The outer arc on the left is mapped by R into regular values of the holomorphicity domain.

In the z-plane there is nothing particular at the critical value λ_{crit}. The ramification points are separate and simple (for pairwise different ϱ_k). The solutions $\omega_{g,n}$ are analytic in λ_{crit} and translate to preimages $\Omega_n^{(g)}(\zeta_1, \ldots, \zeta_n)$ which for $\zeta_i \in \mathcal{V}$ (see Figure 6) are also analytic in λ_{crit}.

What happens is the following. Fix $\zeta_2, \ldots, \zeta_n$ and assume $2g + n > 0$. Then the function $\zeta_1 \mapsto \Omega_n^{(g)}(\zeta_1, \ldots, \zeta_n)$ can be continued to a larger domain $\tilde{\mathcal{V}} \supset \mathcal{V}$ which can come close to $R(\beta_i)$. For $\lambda < \lambda_{\text{crit}}$, any approach $\zeta_1 \to R(\beta_i)$ from inside $\tilde{\mathcal{V}}$ lets $\Omega_n^{(g)}(\zeta_1, \ldots, \zeta_n)$ approach ∞ for all $i = 1, \ldots, 2d$. For $\lambda \nearrow \lambda_{\text{crit}}$ two pairs of divergent approaches come close and eventually merge at λ_{crit}. For $\lambda > \lambda_{\text{crit}}$ those $R(\beta_j)$ for which $\beta_j, \overline{\beta_j}$ yield the core of the avodado become regular values $R(\beta_j) \in \tilde{\mathcal{V}}$. This picture generalises in obvious manner to any $d > 2$, where several critical values of λ occur at which the discs swallow each other. Figure 13 shows several snapshots for $d = 3$.
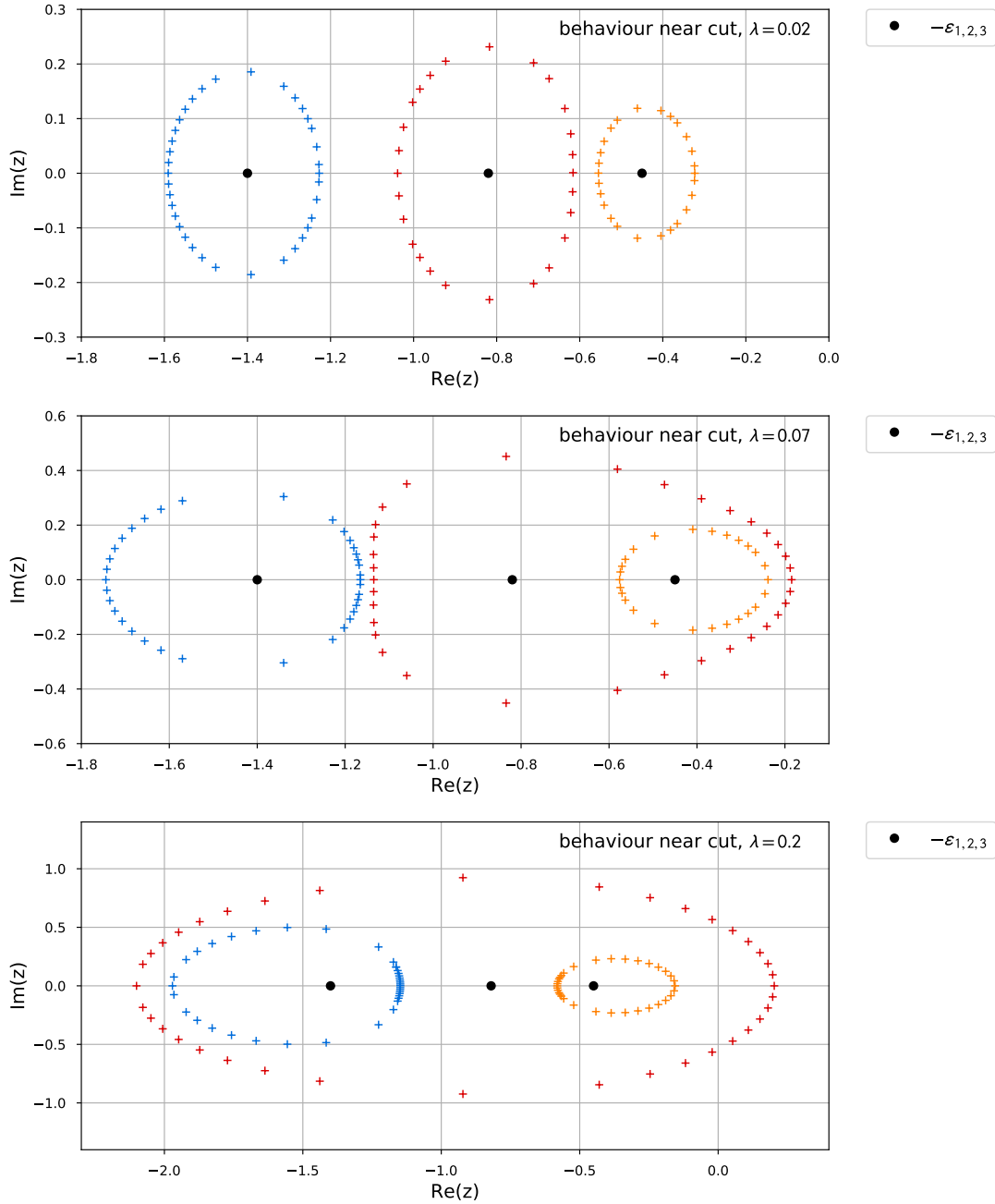
Figure 13. We investigated $d = 3$ with $(\varepsilon_1, \varrho_1) = (0.45, 1)$, $(\varepsilon_2, \varrho_2) = (0.82, 3)$ and $(\varepsilon_3, \varrho_3) = (1.40, 2)$. We see aforementioned $d - 1 = 2$ transitions: At $\lambda = 0.02$, we observe a standard behaviour with three branch cuts. The biggest circle swallows the smallest after a certain threshold value λ_1, this process is finished at $\lambda = 0.07$. In the next transition the second-smallest circle is swallowed at λ_2.

There remains the interesting special case of $\varrho_1 = \varrho_2 = \cdots = \varrho_d$, where the above picture combines with higher-order ramification: Which circle will swallow which? We only mention that there is a multitude of interesting phenomena to be discovered.

7 Conclusion

The quartic analogue of the Kontsevich model offers exceptional possibilities to study structures in quantum field theory. It is a Euclidean quantum field theory defined by deformation of a Gaußian measure. This allows on one hand to derive Dyson–Schwinger equations between the correlation functions, on the other hand to represent these functions as a series in Feynman (ribbon) graphs. What makes this model particular is the possibility to exactly solve the Dyson–Schwinger equations in terms of algebraic or special functions. In this paper we explored the prospects of these achievements for the series of Feynman graphs and investigated transitions between different singularity types when varying the coupling constant.

After these general remarks let us be more precise about what is achieved and what is left for the future. One of the most important aspects of quantum field theory is renormalisation, which entails beautiful mathematical structures [15, 29]. Renormalisation is relevant for systems with infinitely many degrees of freedom. Our model can be extended to infinitely many degrees of freedom; the Dyson–Schwinger equations relate already renormalised correlation functions. The initial non-linear Dyson–Schwinger equation has been solved implicitly [21], but in full generality. An explicit solution in terms of special functions succeeded for the 2D Moyal space (where it gives the Lambert function [31]) and for the 4D Moyal space (where it gives the inverse of a Gauß hypergeometric function [22]). In these two cases all the renormalised correlation functions of disk topology can be written down (thanks to [16]) as integral representations. Expanding them produces the familiar number-theoretical structures of quantum field theory such as multiple zeta values [12] and hyperlogarithms. We remark that the Kontsevich model itself [27] can be treated in a similar manner [20], but the expansion gives at most logarithms.

In this paper we focus on the non-planar sector of the quartic Kontsevich model. Although renormalisation is not needed, the limit to infinitely many degrees of freedom is not yet understood and needs to be studied in the future. All our results apply to a finite-dimensional approximation by $(N \times N)$-matrices. We proved in [10, 26] that all correlation functions are affiliated with a family $\omega_{g,n}(z_1, \ldots, z_n)$ of meromorphic forms which can be explicitly computed by residue techniques. This evaluation becomes increasingly complicated for large (g, n), but the results are remarkably structured and simple. We were led in [10] to the conjecture that the $\omega_{g,n}$ follow blobbed topological recursion [5], i.e., the poles of $z_i \mapsto \omega_{g,n}(z_1, \ldots, z_n)$ at ramification points of R are given by a universal formula. The function R governs the solution [21, 32] of the non-linear Dyson–Schwinger equation.

This paper extends [10] in expressing the coefficients of the $\omega_{g,n}$ as distinguished polynomials in the correlation functions of the quartic Kontevich model (see Propositions 4.7 and 4.8). These distinguished polynomials thus evaluate to expressions much simpler than a correlation function itself (and than any of the factorially many contributing Feynman ribbon graph, see Section 5.3 for their numbers). To unveil this simplicity it was necessary to transform with the inverse of the central function R (see Section 5.2). We remark that the appeerence of the distinguished polynomials is in striking contrast to the Kontsevich model [27] in which the $(1 + \cdots + 1)$-point correlation functions themselves follow topological recursion (see [17, Chapter 6] and [20]). Moreover, the analogue of R in the Kontsevich model is the function $x(z) = z^2 + \text{const}$ with a single ramification point at $z = 0$. We have shown in Section 6 that the dependence of R on the coupling constant leads in the quartic Kontsevich model to a very rich landscape of branch cuts with merge at critical values of the coupling constant. Of course these phenomena are only accessible because we have exact non-perturbative solutions.

After all we have seen that the quartic Kontsevich model shares many features with honest quantum field theories: perturbative expansion into Feynman graphs, non-perturbative formulation via Dyson–Schwinger equations, renormalisation, evaluation into number-theoretical functions. The exact solution found step by step in [10, 21, 31, 32] permits to identify and to explore quantum field-theoretical structures which previously were hidden. Of course these structures could be special to the quartic Kontsevich model. Nonetheless we find it worthwhile to investigate whether something similar could be present also in realistic quantum field theories such as the standard model. Two questions deserve particular attention:

- Is it possible to trace a part of the complexity in QFT back to a change of variables via the complicated inverse of a relatively simple function R?

- Can one collect combinations of the R^{-1}-transformed correlation functions to much simpler functions of topological significance?

Acknowledgements

References

[1] Adler M., van Moerbeke P., A matrix integral solution to two-dimensional W_p-gravity, *Comm. Math. Phys.* **147** (1992), 25–56.

[2] Belliard R., Charbonnier S., Eynard B., Garcia-Failde E., Topological recursion for generalised Kontsevich graphs and r-spin intersection numbers, arXiv:2105.08035.

[3] Bernardi O., Fusy E., Bijections for planar maps with boundaries, *J. Combin. Theory Ser. A* **158** (2018), 176–227, arXiv:1510.05194.

[4] Borot G., Garcia-Failde E., Simple maps, Hurwitz numbers, and topological recursion, *Comm. Math. Phys.* **380** (2020), 581–654, arXiv:1710.07851.

[5] Borot G., Shadrin S., Blobbed topological recursion: properties and applications, *Math. Proc. Cambridge Philos. Soc.* **162** (2017), 39–87, arXiv:1502.00981.

[6] Bouchard V., Eynard B., Think globally, compute locally, *J. High Energy Phys.* **2013** (2013), no. 2, 143, 35 pages, arXiv:1211.2302.

[7] Bouchard V., Hutchinson J., Loliencar P., Meiers M., Rupert M., A generalized topological recursion for arbitrary ramification, *Ann. Henri Poincaré* **15** (2014), 143–169, arXiv:1208.6035.

[8] Bouchard V., Klemm A., Mariño M., Pasquetti S., Remodeling the B-model, *Comm. Math. Phys.* **287** (2009), 117–178, arXiv:0709.1453.

[9] Bouchard V., Mariño M., Hurwitz numbers, matrix models and enumerative geometry, in From Hodge Theory to Integrability and TQFT tt^*-Geometry, *Proc. Sympos. Pure Math.*, Vol. 78, Amer. Math. Soc., Providence, RI, 2008, 263–283, arXiv:0709.1458.

[10] Branahl J., Hock A., Wulkenhaar R., Blobbed topological recursion of the quartic Kontsevich model I: Loop equations and conjectures, arXiv:2008.12201.

[11] Brézin E., Itzykson C., Parisi G., Zuber J.B., Planar diagrams, *Comm. Math. Phys.* **59** (1978), 35–51.

[12] Broadhurst D.J., Kreimer D., Association of multiple zeta values with positive knots via Feynman diagrams up to 9 loops, *Phys. Lett. B* **393** (1997), 403–412, arXiv:hep-th/9609128.

[13] Broadhurst D.J., Kreimer D., Exact solutions of Dyson–Schwinger equations for iterated one loop integrals and propagator coupling duality, *Nuclear Phys. B* **600** (2001), 403–422, arXiv:hep-th/0012146.

[14] Chekhov L., Eynard B., Orantin N., Free energy topological expansion for the 2-matrix model, *J. High Energy Phys.* **2006** (2006), no. 12, 053, 31 pages, arXiv:math-ph/0603003.

[15] Connes A., Kreimer D., Renormalization in quantum field theory and the Riemann–Hilbert problem. I. The Hopf algebra structure of graphs and the main theorem, *Comm. Math. Phys.* **210** (2000), 249–273, arXiv:hep-th/9912092.

[16] de Jong J., Hock A., Wulkenhaar R., Nested Catalan tables and a recursion relation in noncommutative quantum field theory, *Ann. Henri Poincaré*, to appear, arXiv:1904.11231.

[17] Eynard B., Counting surfaces, *Progress in Mathematical Physics*, Vol. 70, Birkhäuser/Springer, Cham, 2016.

[18] Eynard B., Orantin N., Invariants of algebraic curves and topological expansion, *Commun. Number Theory Phys.* **1** (2007), 347–452, arXiv:math-ph/0702045.

[19] Eynard B., Orantin N., Algebraic methods in random matrices and enumerative geometry, arXiv:0811.3531.

[20] Grosse H., Hock A., Wulkenhaar R., A Laplacian to compute intersection numbers on $\overline{\mathcal{M}}_{g,n}$ and correlation functions in NCQFT, arXiv:1903.12526.

[21] Grosse H., Hock A., Wulkenhaar R., Solution of all quartic matrix models, arXiv:1906.04600.

[22] Grosse H., Hock A., Wulkenhaar R., Solution of the self-dual Φ^4 QFT-model on four-dimensional Moyal space, *J. High Energy Phys.* **2020** (2020), no. 1, 081, 16 pages, arXiv:1908.04543.

[23] Grosse H., Wulkenhaar R., Renormalization of noncommutative quantum field theory, in An Invitation to Noncommutative Geometry, World Sci. Publ., Hackensack, NJ, 2008, 129–168, arXiv:0909.1389.

[24] Grosse H., Wulkenhaar R., Self-dual noncommutative ϕ^4-theory in four dimensions is a non-perturbatively solvable and non-trivial quantum field theory, *Comm. Math. Phys.* **329** (2014), 1069–1130, arXiv:1205.0465.

[25] Hock A., Matrix field theory, Ph.D. Thesis, WWU Münster, 2020, arXiv:2005.07525.

[26] Hock A., Wulkenhaar R., Blobbed topological recursion of the quartic Kontsevich model II: Genus = 0, arXiv:2103.13271.

[27] Kontsevich M., Intersection theory on the moduli space of curves and the matrix Airy function, *Comm. Math. Phys.* **147** (1992), 1–23.

[28] Kreimer D., Renormalization and knot theory, *J. Knot Theory Ramifications* **6** (1997), 479–581, arXiv:q-alg/9607022.

[29] Kreimer D., On the Hopf algebra structure of perturbative quantum field theories, *Adv. Theor. Math. Phys.* **2** (1998), 303–334, arXiv:q-alg/9707029.

[30] Mirzakhani M., Simple geodesics and Weil–Petersson volumes of moduli spaces of bordered Riemann surfaces, *Invent. Math.* **167** (2007), 179–222.

[31] Panzer E., Wulkenhaar R., Lambert-W solves the noncommutative Φ^4-model, *Comm. Math. Phys.* **374** (2020), 1935–1961, arXiv:1807.02945.

[32] Schürmann J., Wulkenhaar R., An algebraic approach to a quartic analogue of the Kontsevich model, arXiv:1912.03979.

[33] Witten E., Algebraic geometry associated with matrix models of two-dimensional gravity, in Topological Methods in Modern Mathematics (Stony Brook, NY, 1991), Publish or Perish, Houston, TX, 1993, 235–269.

[34] Zhukovsky N., Über die Konturen der Tragflächen der Drachenflieger, *Z. Flugtechnik Motorluftschiffahrt* **1** (1910), 281–284.